Report No. CG-D-17-98

Nonlinear Time-Domain Simulation of Fishing Vessel Capsizing in Quartering Seas

Woei-Min Lin
Michael J. Meinhold
Nils Salvesen

Ship Technology Division
Science Applications International Corporation
134 Holiday Court, Suite 318
Annapolis, MD 21401

FINAL REPORT
April 1998

Prepared for:

U.S. Department of Transportation
United States Coast Guard
Marine Safety and Environmental Protection, (G-M)
Washington, DC 20593-0001

and

U.S. Coast Guard
Research and Development Center
1082 Shennecossett Road
Groton, CT 0634-6096

NOTICE

This document is disseminated under the sponsorship of the Department of Transportation in the interest of information exchange. The United States Government assumes no liability for its contents or use thereof.

The United States Government does not endorse products or manufacturers. Trade or manufacturers' names appear herein solely because they are considered essential to the object of this report.

The contents of this report reflect the views of the Coast Guard Research & Development Center. This report does not constitute a standard, specification, or regulation.

Marc B. Mandler
Technical Director
United States Coast Guard
Research & Development Center
1082 Shennecossett Road
Groton, CT 06340-6096

Technical Report Documentation Page

1. Report No. CG-D-17-98	2. Government Accession No.	3. Recipient's Catalog No.

4. Title and Subtitle

Nonlinear Time-Domain Simulation of Fishing Vessel Capsizing in Quartering Seas

5. Report Date
April 1998

6. Performing Organization Code
Project No. 3301.01.02

7. Author(s)
Woei-Min Lin, Michael J. Meinhold and Nils Salvesen

8. Performing Organization Report No.
R&DC 10/98

9. Performing Organization Name and Address
Ship Technology Division
Science Applications International Corporation
134 Holiday Court, Suite 318
Annapolis, MD 21401

10. Work Unit No. (TRAIS)

11. Contract or Grant No.
MIPR No. Z51100-9-0007

12. Sponsoring Agency Name and Address
U.S. Department of Transportation
United States Coast Guard
Marine Safety and Environmental
Protection, (G-M)
Washington, DC 20593-0001

U.S. Coast Guard
Research and Development Center
1082 Shennecossett Road
Groton, CT 06340-6096

13. Type of Report and Period Covered
Final Report

14. Sponsoring Agency Code
Commandant (G-MSE)
U.S. Coast Guard Headquarters
Washington, DC 20593-0001

15. Supplementary Notes
The R&DC technical point of contact is James White, 860-441-2734.

16. Abstract (Maximum 200 words)

Ship design practice has been to measure stability by static criteria and to compensate for dynamic effects through a margin of safety. However, there is a fundamental difference between static and dynamic stability. Certain factors that result in favorable static stability characteristics may actually present greater danger when considered in light of a dynamic analysis. Traditional linear strip-theory methods are not suitable for assessing ship capsizing.

The main objective of the present project has been to investigate the capabilities of the 3-D nonlinear time-domain Large-Amplitude Motion Program (LAMP) for the evaluation of fishing vessels operating in extreme waves. The project's focus was building upon the previous LAMP development and extending it to the modeling of maritime casualties, including a time-domain simulation of a ship capsizing in stern quartering seas. This modeling capability will allow both the analysis of recorded casualties and the identification of potential safety concerns.

17. Key Words		18. Distribution Statement
capsize	ship motions	This document is available to the U.S. public through the National Technical Information Service, Springfield, VA 22161.
seakeeping	stability	
nonlinear	IDEAS	

19. Security Classif. (of this report)	20. SECURITY CLASSIF. (of this page)	21. No. of Pages	22. Price
UNCLASSIFIED	UNCLASSIFIED		

Form DOT F 1700.7 (8/72) Reproduction of form and completed page is authorized

METRIC CONVERSION FACTORS

Approximate Conversions to Metric Measures

Symbol	When You Know	Multiply By	To Find	Symbol
	LENGTH			
in	inches	* 2.5	centimeters	cm
ft	feet	30	centimeters	cm
yd	yards	0.9	meters	m
mi	miles	1.6	kilometers	km
	AREA			
in^2	square inches	6.5	square centimeters	cm^2
ft^2	square feet	0.09	square meters	m^2
yd^2	square yards	0.8	square meters	m^2
mi^2	square miles	2.6	square kilometers	km^2
	acres	0.4	hectares	ha
	MASS (WEIGHT)			
oz	ounces	28	grams	g
lb	pounds	0.45	kilograms	kg
	short tons (2000 lb)	0.9	tonnes	t
	VOLUME			
tsp	teaspoons	5	milliliters	ml
tbsp	tablespoons	15	milliliters	ml
fl oz	fluid ounces	30	milliliters	ml
c	cups	0.24	liters	l
pt	pints	0.47	liters	l
qt	quarts	0.95	liters	l
gal	gallons	3.8	liters	l
ft^3	cubic feet	0.03	cubic meters	m^3
yd^3	cubic yards	0.76	cubic meters	m^3
	TEMPERATURE (EXACT)			
°F	Fahrenheit temperature	5/9 (after subtracting 32)	Celsius temperature	°C

*1 in = 2.54 (exactly).

Approximate Conversions from Metric Measures

Symbol	When You Know	Multiply By	To Find	Symbol
	LENGTH			
mm	millimeters	0.04	inches	in
cm	centimeters	0.4	inches	in
m	meters	3.3	feet	ft
m	meters	1.1	yards	yd
km	kilometers	0.6	miles	mi
	AREA			
cm^2	square centimeters	0.16	square inches	in^2
m^2	square meters	1.2	square yards	yd^2
km^2	square kilometers	0.4	square miles	mi^2
ha	hectares (10,000 m^2)	2.5	acres	
	MASS (WEIGHT)			
g	grams	0.035	ounces	oz
kg	kilograms	2.2	pounds	lb
t	tonnes (1000 kg)	1.1	short tons	
	VOLUME			
ml	milliliters	0.03	fluid ounces	fl oz
l	liters	0.125	cups	c
l	liters	2.1	pints	pt
l	liters	1.06	quarts	qt
l	liters	0.26	gallons	gal
m^3	cubic meters	35	cubic feet	ft^3
m^3	cubic meters	1.3	cubic yards	yd^3
	TEMPERATURE (EXACT)			
°C	Celsius temperature	9/5 (then add 32)	Fahrenheit temperature	°F

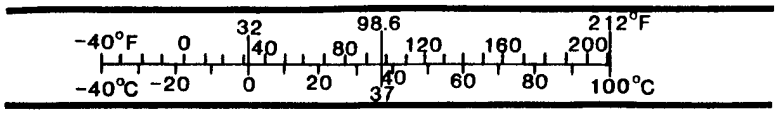

Acknowledgments

This study has been sponsored by the U.S. Coast Guard Research and Development Center, Groton, Connecticut. We appreciate the interest and enthusiastic support of Mr. James A. White. The funding has been provided through a contract with the Office of Naval Research (Dr. Edwin Rood) as part of a much larger development effort of the Interactive Design, Evaluation, and Assessment System (IDEAS). The total IDEAS system has been developed under the joint sponsorship of the U.S. Coast Guard, ARPA (Advanced Research Project Agency), ONR (Office of Naval Research), NAVSEA (Naval Sea Systems Command), and ABS (American Bureau of Shipping). We would like to thank Mr. Kenneth Weems for his help in developing the LAMP System and preparing the time-domain animation plots shown in this report. We would also like to thank Mr. Thomas Treakle and Ms. Marian Weems for their help in preparing the final version of this report.

Table of Contents

Lists of Figures and Tables

Nomenclature

ABS	American Bureau of Shipping
ARPA	Advanced Research Project Agency
IDEAS	Interactive Design, Evaluation, and Assessment System
LAMP	SAIC's Large-Amplitude Motion Program
ONR	Office of Naval Research
NAVSEA	Naval Sea Systems Command
PID	proportional, integral, and derivative rudder control algorithm
RANS	Reynolds Averaged Navier Stokes full viscous flow codes
SMP	U.S. Navy's Ship Motion Program code
USCG	U.S. Coast Guard
α	angle of attack
α_{stall}	limiting angle of attack
α_{trail}	stall angle if flow is at a small angle to the trailing edge, so the foil is assumed to be lifting "backwards"
A_m	maximum rudder angle
A_R	aspect ratio
b_{44V}	roll damping due to skin friction with forward speed
C	effective chord of foil
$\vec{C}$	average chord direction from tail to nose
C_A	coefficient of normal pressure magnification
C_f	frictional coefficient
C_K	hull form correction
C_N	coefficient of normal pressure
C_S	factor for bilge keels built up from plates
CG	center of gravity
δ_c	rudder command
$F(t)$	incident wave surface
g	gravitational acceleration
G_a	gain coefficient for the proportional term
G_b	gain coefficient for the derivative term
h	wave height
$h_{1/3}$ or $H_{1/3}$	significant wave height
$\overline{\eta_4}$	roll amplitude
$\overline{\dot{\eta}_4}$	roll velocity amplitude
$\eta_4(t)$	time-dependent roll angle
$\dot{\eta}_4(t)$	time-dependent roll velocity
L	ship length
λ	wavelength
M	moment
P_B	proportional band
$\vec{P}_{foil}$	location of foil center
ρ	water density
r_s	"equivalent" radius
R_m	slew rate
$\vec{R}_{ship}$	ship rotation rate about local origin
S	effective span of foil
$\vec{S}$	ship rotation rate about local origin
S_{lift}	direction of lift influence
$S(\omega)$	amplitude spectrum for the seaway
Δt	time step size
T_0	modal period (wave period at which $S(\omega)$ is maximum)
U	ship speed
$\vec{U}_{ship}$	velocity of ship at local origin
$\vec{v}_e$	direction of incident flow
$\vec{V}$	fluid velocity at foil center
V_N	normal flow
ψ	ship heading

Executive Summary

Ship design practice has been to measure stability by static criteria and to compensate for dynamic effects through a margin of safety. However, there is a fundamental difference between static and dynamic stability. The Fastnet Yacht Race disaster in 1979 revealed that "certain factors which result in favorable static stability characteristics may actually present greater danger when considered in light of a dynamic analysis" (Stephens, Kirkman and Peterson, 1981).

The existing linear strip-theory method cannot be used for assessing capsizing. Advanced nonlinear simulation methods are required. As we shall see, such advanced methods are now under development and their application to the assessment of the vessel dynamic stability problem is a realistic practical goal today.

The main objective of the present project has been to investigate the capabilities of the 3-D nonlinear time-domain Large-Amplitude Motion Program (LAMP) for the evaluation of fishing vessels operating in extreme waves. The project's focus was building upon the previous LAMP development and extending it to the modeling of maritime casualties, including a time-domain simulation of a ship capsizing in stern quartering seas. This modeling capability will allow both the analysis of recorded casualties and the identification of potential safety concerns.

Ship motions in stern quartering seas are extremely complicated since the roll motion is highly nonlinear and the viscous effects are important. A typical example of stern quartering sea capsizing is illustrated in a time sequence in Figure 1. The simulations are for the 70-foot (21.3 m) fishing vessel *Italian Gold* with a heavy loading condition in regular stern quartering seas. The center of gravity, CG, of the ship is located at the mid ship and 0.27 ft (0.08 m) above the load waterline. A linear moderate wave (wave height, h=6 ft [1.8 m], and wavelength λ=100 ft [30.5 m]) approaches from the stern quarter in the starboard direction. The simulation shows that operating with a course-keeping autopilot, the ship turns into almost beam sea condition and capsizes in the direction of wave propagation.

In this report, the methodology used to assess vessel stability and safety is discussed. It emphasizes the importance of performing analyses of dynamic stability rather than applying margins of safety to static stability criteria. The need for computational tools for accurate stability and safety assessment is addressed.

Using the current LAMP code, the present study shows some examples of fishing boat capsizings in seas that are initially off the stern quarter. These results clearly demonstrate the necessity and power of a nonlinear time-domain simulation tool for the study of vessel stability and for the assessment of ship safety. However, an extensive validation study and possibly further improvements to the present method may be required for accurate predictions of extreme ship motions in more general extreme sea conditions.

Time = 8.01

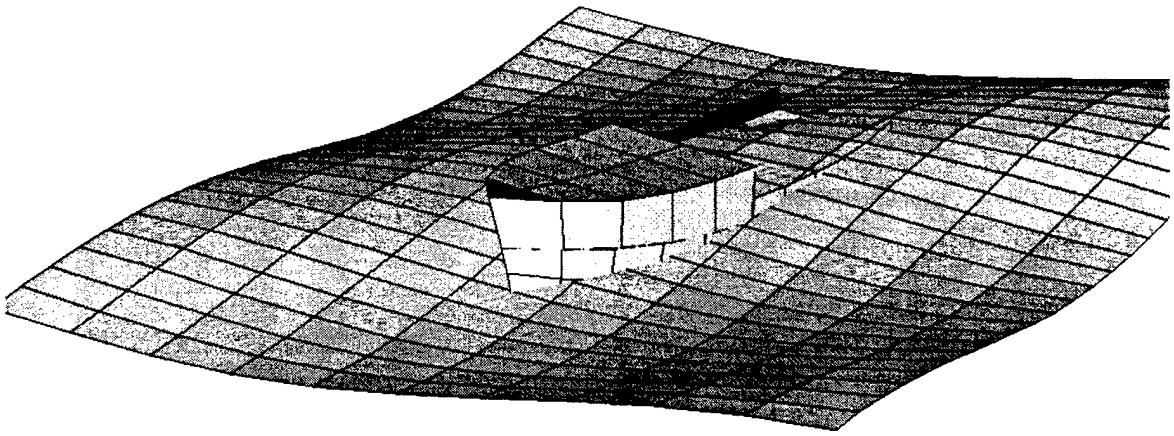

Time = 9.00

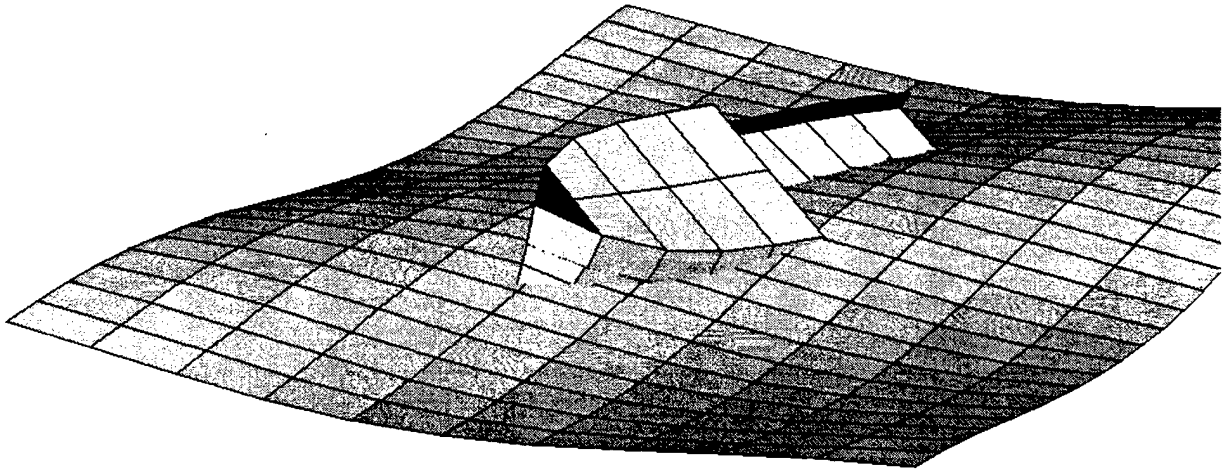

Time = 9.99

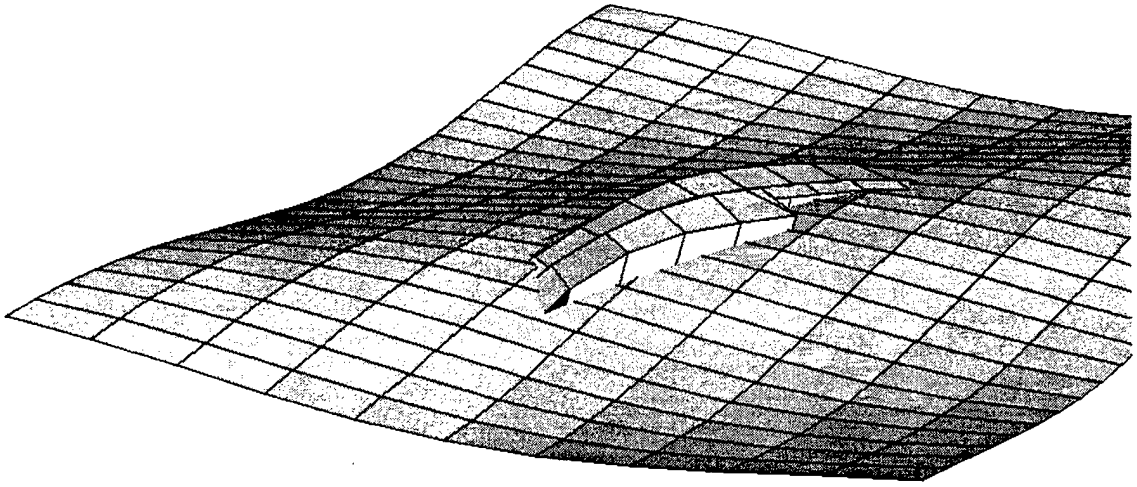

Figure 1. Example of the Fishing Vessel *Italian Gold* Capsizing in Large-Amplitude Regular Stern Quartering Waves

1 Introduction

One of the primary missions of the U.S. Coast Guard is the protection of life and property by the establishment and enforcement of marine safety standards. The ideal standard seeks to ensure safety without unduly affecting the ship's operability. A major safety concern is the prevention of the loss of life and property due to ship capsizing. Current regulations seek to prevent such occurrences by setting minimum stability and freeboard requirements. These regulations are based mainly on hydrostatics. They were developed from an analysis of, and experience with, traditional ship configurations.

The stability assessment of new, innovative ship forms and the assessment of capsizing accidents often require very expensive and time consuming experiments. The existing ship motion prediction tools are primarily based on hydrostatics and linear strip theory, which can only be used for assessing small amplitude motions in moderate sea conditions. Therefore, an accurate ship motion simulation method may have a large impact on ship safety assessment.

Computational simulation techniques and computer architectures have finally reached such a level of sophistication that the development of a simulation system for vessel stability and safety assessment for extreme seas is a practical goal. The purpose of this report is to discuss the recent advances in computational hydrodynamics research and the related practical engineering systems, in particular the LAMP System (Lin and Yue, 1990, Lin, *et al.*, 1992, 1993, 1994), for the assessment of the stability and safety of a vessel operating in extreme seas.

Since stability criteria are primarily based on static stability, it is extremely important to emphasize that the physics governing static stability is quite different from the physics for dynamic stability. To illustrate this point, we shall first look at a sailing yacht disaster which has been investigated extensively and which is quite well understood.

1.1 Dynamic vs. Static Stability

The Fastnet Race of 1979 is considered to be the greatest disaster in the history of the sport of yachting. Seventy-seven boats were completely capsized and fifteen sailors died (Rousmaniere, 1980). Stephens, Kirkman and Peterson (1981) analyzed the Fastnet disaster in their landmark paper on "Sailing Yacht Capsizing". They addressed the capsize mechanism, the environmental conditions, and the design approach which led to the terrible disaster. They pointed out that design practice has been to measure stability by static criteria and to compensate for dynamic effects through margins of safety. Their investigation of the Fastnet Race disaster revealed that " certain factors which result in favorable static stability characteristics may actually present greater danger when considered in light of a dynamic analysis."

This is a very important aspect of vessel stability that unfortunately is often overlooked in setting safety requirements. For example, it is often assumed that a vessel's stability is a function of its freeboard with larger freeboard providing greater capsizing resistance. This is correct from a static point of view, but Stephens, *et al.*, showed that the dynamics of the single wave impact capsizing

mechanism which dominated the Fastnet '79 casualties (see Figure 2) had the opposite effect. They asserted that:

> ...freeboard, which helps raise the zero-stability crossing in a static case and hence appears as safe, is the source of much overturning energy being impacted to the yacht due to the large area being struck by the breaker and the increased moment arm acting for overturn.

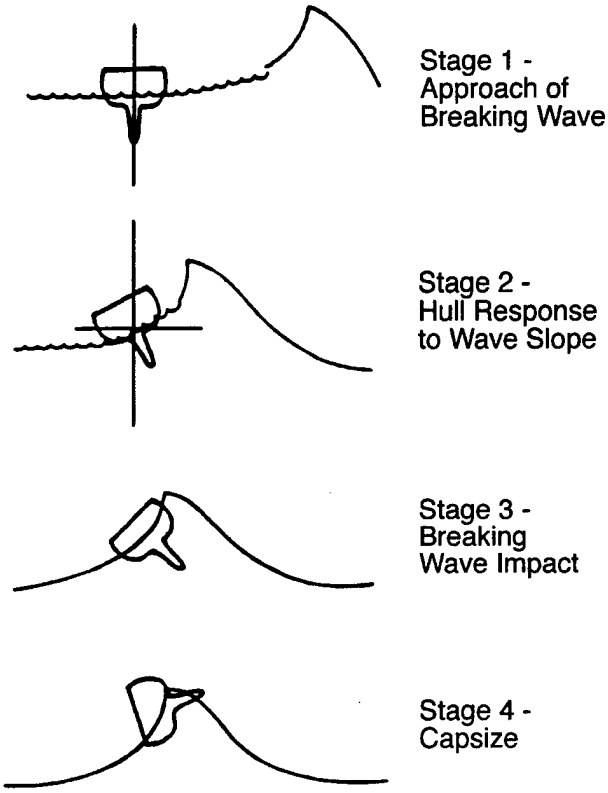

Figure 2. Schematic of the Single Wave Impact Capsizing that Dominated the Fastnet '79 Casualties (from Stephens, *et al.*, 1981)

Furthermore, Stephens, *et al.*, concluded that

> ...the beam contribution to static stability is washed out in a capsize by a corresponding moment caused by local wave slope.

The reason for reviewing the Fastnet Race disaster is to stress the importance of analyzing dynamic stability in extreme sea conditions and to focus attention on the fact that there is a fundamental difference between static and dynamic stability. Vessel safety requirements cannot be established by considering static stability alone and then applying some safety factor to include dynamic aspects. Design trends driven by static stability requirements resulted in a catastrophic disaster in the Fastnet Race of 1979 because they increased freeboard and increased beam, causing dynamic stability problems.

1.2 Summary of Present Study

In this report, we address the research, development, and application of advanced computational methods for the assessment of dynamic stability in a seaway. As an example, we use the LAMP system to study a particular casualty: the capsize of the stern dragger *Italian Gold* in a storm off Massachusetts in September of 1994. The intent of this exercise was two-fold :

- To attempt to learn more about the dynamic mechanisms causing capsizing in statically stable vessels.
- To test and improve the LAMP system for application to such casualty analysis.

Two features which were recently added to LAMP have made it possible to do these analyses in other than head-seas conditions: the ability to calculate viscous forces including roll and appendage lift, and a dynamic automatic control system for steering. This challenging real-world problem provided an opportunity to test these features and improve them.

Static stability is assumed to be well understood. It is important to recognize that the advanced computational hydrodynamic tools discussed in this report are equally important for addressing all of the following problems related to vessel safety in waves:

- Dynamic Stability Structural
- Equipment Damage
- Crew Safety.

However, in this report, we focus on the dynamic stability problem. Stability as it is discussed here will include both intact and damaged stability.

The development of computational tools for dynamic vessel stability must be considered as a portion of the much larger topic of seakeeping. Seakeeping assessment, which includes both the wave-induced motions and hydrodynamic loads, may be divided into two classes:

- Linear frequency-domain predictions
- Nonlinear time-domain simulations.

Linear frequency-domain prediction methods (*i.e.* Strip Theory) have been extremely successful in determining sea state operability limitations for weapon systems on naval vessels (Kennel, 1985). Such methods have also been useful in estimating the wave-induced loads for large ships (Liu, *et al.*, 1992). However, the linear "strip theory" tools are based upon the assumption that both the motions and the wave amplitudes are small relative to the vessel's dimensions (in particular the draft). Furthermore, many linear methods assume wall sidedness. These are serious limitations - the assumptions are not valid in general for vessel response in extreme seas.

Nonlinear time-domain simulation is required to determine the vessel's response in extreme seas. Because of this requirement, dynamic stability predictions are an order of magnitude more complex than linear frequency-domain predictions. For example, the wave field description for extreme response prediction must contain much more detailed information than the wave energy-spectrum representation used for linear prediction.

In order to obtain the probabilistic estimates needed for setting safety standards, one has to apply a combination of deterministic and probabilistic calculations. The assessment of a vessel's dynamic stability in waves may be divided into three parts:

- **Wave-Event Modeling:** extreme wave characterization, selection of potentially dangerous extreme wave events, and detailed numerical modeling of the complex nonlinear hydrodynamics aspects of the selected wave events
- **Vessel-Response Simulations:** an accurate time-domain simulation of the vessel's response to the selected wave events
- **Probabilistic Predictions:** an estimate of the probability of occurrence of the wave/vessel encounters that will result in catastrophic responses.

The importance and development of these three parts have been addressed by Salvesen and Lin (1993) in their proposed SAFE SEAS System. The first and the third parts will not be discussed further in this report. The current development of the vessel-response simulations will be discussed here.

Section 2 of this report gives a general description of the LAMP System used for the current simulation study. Section 3 describes the hull form studied and the hydrostatic characteristics of the vessel. Results of using the LAMP system in nonlinear simulation of ship capsizing in stern quartering seas are presented in Section 4. Both time-domain simulations and some of the mechanism that causes the ship to capsize in stern quartering seas will be given.

2 The LAMP System

2.1 The LAMP Approach

In 1990, Lin and Yue presented a three-dimensional time-domain method to study large-amplitude motions and loads of floating bodies in waves. In their so-called "body-exact" approach, the free-surface boundary conditions are linearized and the body boundary condition is satisfied exactly on the portion of the instantaneous wetted surface that lies below the undisturbed free surface. The problem is solved using a transient free-surface Green's function singularity distribution. The validity and practical utility of this method has been demonstrated by several studies, including predictions of large-amplitude motion coefficients, motion history of a ship advancing in an irregular seaway, and the effect of bow flare on wave loads (see Lin and Yue 1990, 1992; Lin *et al.*, 1991, 1992).

In 1993, Lin and Yue extend the applicability of their method to allow ship motions in more severe wave conditions in which both the body motions and the incident waves can be large. In this new Large-Amplitude Motion Program, LAMP, the body boundary condition is satisfied on the instantaneous wetted surface below the incident wave profile with the assumption that the diffracted waves are small compared to the incident wave and that the incident wave slopes are small. At each time step, local incident free surface elevations are used to transform the body geometry into a computational domain with a deformed body and a flat free surface. By linearizing the free surface boundary conditions about this incident wave surface, the problem can be solved in the computational domain using linearized free-surface transient Green's functions. The two main features of this new large-amplitude approach are:

1. true hydrodynamic effects for the wetted portion of the ship under the incident wave surface
2. automatic inclusion of the correct hydrostatic and Froude-Krylov forces.

A summary of this new approach is given in Lin *et al.* (1994).

The LAMP approach solves the six-degree-of-freedom dynamical equations of motion in the time domain for motion simulation. At each time step, forces and moments acting on the body are given. For solving ship motion problems in oblique seas, viscous and lifting forces are important. A brief description of the viscous force calculations included in the LAMP approach is given in the next section.

In the LAMP code, the seaway is represented by summation of linear wave components. The seaway can be specified as either regular (single component) or a random wave (multiple components) specified by a wave spectrum. A discussion of the seaway representation is given later in this section. For motion simulation of fishing vessel in stern quartering seas, course-keeping rudder control is used. A simple proportional, integral, and derivative (PID) control of the rudder is implemented in the LAMP code. This control algorithm is discussed briefly also later in the section.

2.2 Viscous Forces in the Time Domain

2.2.1 Overview

In oblique or beam seas, forces due to viscous and lift effects will have a significant effect on the motions and loads. LAMP includes an option to approximate some of these effects in the time-domain. These included effects may not completely characterize the viscous flow separation effects present in maneuvering cases. Further development using full viscous flow codes such as Reynolds Averaged Navier Stokes (RANS) solvers may be necessary to better characterize the 3-D flow effects found in maneuvering cases. The viscous and lift effects approximated are as shown in Table 1. For each effect, the table presents a reference for the calculation method and whether it is a linear or non-linear effect. These components are determined in a manner very similar to that used in the U.S. Navy's Ship Motion Program (SMP) code (Meyers, *et al.*, 1981) . However, in the SMP code, forces are calculated in the frequency domain, assuming certain averaged magnitudes of roll displacement and roll velocity.

Such an averaged roll damping approach is not satisfactory for time domain calculations where a primary objective is the accurate calculation of the extreme response events. The new calculation method uses the formulae from the references in Table 1, but uses the current magnitude of roll displacement and roll velocity rather than an averaged value. At every time step, the time history of roll displacement and roll velocity is examined for a peak value, positive or negative. These peak values generate parameters for the viscous forces until a new peak is found. At any given time step, the actual forces depend on these parameters and the instantaneous value of roll displacement and roll velocity. This approach is very different from the approach used in SMP, which uses an iterative process to calculate an "equivalent" or "averaged" roll amplitude for viscous damping. The current approach is a more direct calculation taking advantage of the fact that the roll angle and velocity are known at all time.

Table 1. Viscous and Lift Effects

Effect	Reference	Linearity
Hull Lift	Himeno (1981)	Linear
Skeg, Bilge Keel, and Foil Lift	Himeno (1981)	Linear
Hull Eddy-Making	Tanaka (1960) and Ideda *et al.* (1978)	Non-Linear
Bilge Keel Eddy-Making	Kato (1966)	Non-Linear
Skeg and Foil Eddy-Making	Tanaka (1960), Ideda *et al.* (1978), and Tamiya (1972)	Non-Linear
Hull Skin Friction	Kato (1966)	Non-Linear

2.2.2 Lift Forces

A lift force is calculated for every foil, including the hull and bilge keels. In the following discussion, all the values are described in a coordinate system fixed to the ship. Assume we have determined the ship motion and the fluid flow in this system:

$\vec{U}_{ship}$ = velocity of ship at local origin
$\vec{R}_{ship}$ =ship rotation rate about local origin

We know the following information about the foil:

$\vec{S}$ = ship rotation rate about local origin
$\vec{C}$ = average chord direction from tail to nose
$\vec{P}_{foil}$ = location of foil center
$\vec{V}$ = fluid velocity at foil center

Then we can determine the relative velocity at the foil center, as follows:

$$\vec{V}_R = \vec{V} - (\vec{U}_{ship} + \vec{R}_{ship} \times \vec{P}_{foil}) \tag{1}$$

We normalize these three vectors as:

$$\vec{s} = \frac{\vec{S}}{\left|\vec{S}\right|}$$

$$\vec{c} = \frac{\vec{C}}{\left|\vec{C}\right|}$$

$$\vec{v}_R = \frac{\vec{V}_R}{\left|\vec{V}_R\right|}$$

To find the velocity for the lift calculation, we determine the component of velocity in the span direction, and subtract it from the total relative velocity.

$$\vec{V}_e = \vec{V}_R - \vec{s}(\vec{V}_R \cdot \vec{s}) \tag{2}$$

We find the unit flow direction as

$$\vec{v}_e = \frac{\vec{V}_e}{\left|\vec{V}_e\right|} \tag{3}$$

The unit lift direction is perpendicular to this effective flow and the span direction,

$$\vec{l} = \vec{v}_e \times \vec{s} \tag{4}$$

The effective angle of attack is the angle between the flow vector and the chord tail-to-nose vector. This is a rough approximation that that works well for rectangular shapes and is sufficient for the purposes of this formulation. The vectors $\vec{v}_e$ and $\vec{c}$ are normalized, so the cosine of the angle of attack α is the dot product of the two:

$$\alpha = \cos^{-1}(\vec{v}_e \cdot \vec{s}) \tag{5}$$

The lift coefficient is determined as a function of the aspect ratio A_R. In all cases, the foils are assumed to be "groundboarded," with the effect of doubling the geometric aspect ratio. The effective aspect ratio is then

$$A_R = \frac{2S}{C} \tag{6}$$

where: S = effective span of foil
C = effective chord of foil

This is the result of Prandt's lifting line theory and is sufficient for the purposes of these calculations. Then the lift-curve slope is:

$$C_{L\alpha} = \frac{\pi}{2} A_R \qquad \text{if } A_R < 2.0 \tag{7}$$

$$C_{L\alpha} = \frac{2\pi}{1 + \frac{2}{A_R}} A_R \qquad \text{if } A_R \geq 2.0 \tag{8}$$

The foil is assumed to have this lift-curve slope up to a limiting angle of attack, α_{stall}. Above this angle, the lift goes to zero. If the flow is at a small angle to the trailing edge, the foil is assumed to be lifting "backwards" and has a different stall angle, α_{trail}.

The lift coefficient is:

$$\begin{aligned}
C_L &= C_{l\alpha} \cdot \alpha \left|V_e\right| \ (S \cdot C) &&: \quad |\alpha| < \alpha_{stall} \\
C_L &= C_{l\alpha} \cdot (\pi - \alpha) \left|V_e\right| \ (S \cdot C) &&: \quad |\pi - \alpha| < \alpha_{trail} \\
C_L &= 0.0 &&: \quad \alpha_{stall} < \alpha < \pi - \alpha_{stall} \\
C_L &= 0.0 &&: \quad -\pi + \alpha_{trail} < \alpha < -\alpha_{stall}
\end{aligned} \tag{9}$$

In the current program, the stall angles are as follows:

	Foils	Hull	Bilge Keels
α_{stall}	24	12	12
α_{trail}	12	12	12

To properly orient the lift vector, its direction relative to the lifting surface must be the same as the normal component of the incident velocity. To determine this, we take the sign of the dot product,

$$S_{lift} = sign(\vec{v}_e - \vec{c}(\vec{v} \cdot \vec{c}) \cdot \vec{l}) \tag{10}$$

where S_{lift} = the direction of the lift influence

The lift vector is then

$$\vec{L} = S_{lift} \vec{l} \frac{1}{2} C_l \rho \left| \vec{V}_e \right|^2 SC \tag{11}$$

where ρ = density of water.

In the current version of LAMP, the velocity on the appendages does not include the wave particle velocities, but can include a velocity increment to simulate the effects of the propeller wash. However, this velocity increment was not available in LAMP when these calculations were performed.

2.2.3 Effect of Eddy-Making Forces on Roll

The eddy-making force is calculated as the force on a flat plate in a flow normal to its surface. This is the time-domain equivalent of the semi-empirical methods used in SMP, developed by Kato (1966).

First we find the normal flow, V_N, as

$$V_N = V \cdot (\vec{c} \times \vec{s}) \tag{12}$$

The Reynolds number based on the span is

$$R_E = \frac{V_N S}{\nu} \tag{13}$$

The "coefficient of normal pressure," C_N, is calculated (after Kato) as

$$
\begin{aligned}
C_N &= 1.98\exp -11.0\tfrac{S}{C} &&: && \tfrac{S}{C} < 0.07 \\
C_N &= 1.98\exp -11.0\tfrac{C}{S} &&: && \tfrac{C}{S} < 0.07 \\
C_N &= 1.18 &&: && 0.07 \le \tfrac{S}{C} \le \tfrac{1}{0.07}
\end{aligned} \qquad (14)
$$

The "normal pressure magnification," C_A, is calculated (after Kato) as

$$
\begin{aligned}
C_A &= 1.95 - 0.25\ln(R_E) + 0.20\sin(\tfrac{\pi}{0.54}(\ln(R_E) - 2.19)) &&: && R_E < 1000 \\
C_L &= 1.0 &&: && R_E \ge 1000
\end{aligned} \qquad (15)
$$

The hull form correction, C_K, and the factor for bilge keels built up from plates, C_S, are both set to 1.0. The normal or eddy-making force is then calculated as:

$$
\vec{E} = (\vec{c} \times \vec{s})\frac{1}{2} C_N C_S C_A C_K \rho V_n^{\,2} SC \qquad (16)
$$

Any drag force can be calculated and has the direction of the incident flow, $\vec{v}_e$. In the current implementation, the flat-plate skin friction drag is calculated using the local Reynolds number.

2.2.4 Effect of Hull Skin Friction on Roll

The following derivation shows how the semi-empirical frequency domain techniques are applied to the time-domain problem. Kato (1958) established a semi-empirical technique for estimating this component. His formulae expressed the damping as a roll decrement ratio for zero forward speed. Further work by Tamiya (1972) added the effect of speed, and Himeno summarized this work in 1981, expressing the damping coefficient as follows:

$$
b_{44V} = (1 + 4.1\frac{U}{\omega L})(\frac{1}{2}\rho S r_s^{\,3} C_f \overline{\dot{\eta}_4}) \qquad (17)
$$

where

b_{44V}	=	the roll damping due to skin friction with forward speed
U	=	ship speed
L	=	ship length
ω	=	roll frequency
ρ	=	water density
S	=	surface area
r_s	=	"equivalent" radius
C_f	=	frictional coefficient
$\overline{\eta_4}$	=	roll amplitude
$\overline{\dot{\eta}_4}$	=	roll velocity amplitude
$\eta_4(t)$	=	time-dependent roll angle
$\dot{\eta}_4(t)$	=	time-dependent roll velocity

We write the frequency-domain moment amplitude as the product of the damping coefficient and the roll velocity magnitude:

$$M_{44V} = (1+4.1\frac{U}{\omega L})(\frac{1}{2}\rho S r_s^3 C_f \overline{\dot{\eta}_4}^2) \tag{18}$$

In the quasi-steady approach, we vary both the damping coefficient and the roll velocity with time. To use the frequency-domain data, we need to choose an appropriate value for the magnitudes $\overline{\eta_4}$ and $\overline{\dot{\eta}_4}$. At every time step, we check the value of $\eta_4(t)$ and $\dot{\eta}_4(t)$ to see if they have passed through zero. If they have, we take the previous maximum as the new value of the roll magnitude. At every time step, we calculate the moment as

$$M_{44V}(t) = (1+4.1\frac{U}{\omega L})(\frac{1}{2}\rho S r_s^3 C_f \overline{\dot{\eta}_4}\dot{\eta}_4(t)) \tag{19}$$

This is the procedure followed at every time step i to track the value of the roll magnitudes:

1. If the sign of η_{4i} does not equal the sign of η_{4i-1}, find $\overline{\eta_4}$ as the maximum since the last zero crossing
2. If the sign of $\dot{\eta}_{4i}$ does not equal the sign of $\dot{\eta}_{4i-1}$, find $\overline{\dot{\eta}_4}$ as the maximum since the last zero crossing
3. Calculate $M_{44V}(t)$.

2.3 Seaway Description

2.3.1 Overview

The seaway definition used in the LAMP system allows any discrete set of waves to be superimposed. The program LAMP seaway module allows the user to generate one of these sets based on parameters using standard spectral seaway definitions found from empirical data. The user defines the power spectrum of the seaway with either the Brettschneider Two-Parameter Spectrum, which uses the significant wave height and the modal period, or the Pierson-Moskowitz one-parameter spectrum, which uses only the significant wave height.

2.3.2 Brettschneider Two-Parameter Spectrum

The user supplies the modal period and significant wave height of the seaway.

The Brettschneider Power Spectrum is evaluated as follows:

$$S(\omega) = 486.00 * H_{\frac{1}{3}}^2 * T_0^{-4} * \omega^{-5} * e^{-1948.18 * T_0^{-4} \omega^{-4}} \tag{20}$$

where ω = wave frequency
T_0 = modal period (wave period at which $S(\omega)$ is maximum)
$H_{\frac{1}{3}}$ = significant wave height
$S(\omega)$ = amplitude spectrum for the seaway.

2.3.3 Pierson-Moskowitz One-Parameter Spectrum

If a Pierson-Moskowitz spectrum is chosen, only the significant wave height is input, and the modal period is calculated as below. Note that the Pierson-Moskowitz formula is generally based on wind speed, but that there assumes the following direct relationship between wind speed and significant wave height.

$$H_{\frac{1}{3}} = \frac{U_2}{g}\sqrt{\frac{16.034*0.0081}{4*0.74}} \tag{21}$$

where U is the wind speed 10 meters above the free surface.

Then, if $H_{\frac{1}{3}}$ is either input or calculated based on U, the modal period T_0 can be calculated as follows:

$$T_0 = \frac{2\pi}{gk}\sqrt{\frac{H_{\frac{1}{3}}\sqrt{5}}{\alpha}} \tag{22}$$

where g = gravitational acceleration
k = 4.00043
α = 0.0081, Phillips Constant.

2.3.4 Discretization and Simulation of a Time-Domain Wave

In order to discretize the spectrum, the program has the user input the number of waves to use and chooses the number of waves to define the seaway. The frequencies are determined by a geometric spreading away from the modal frequency in both directions. Half of the specified numbers are used for frequencies below the modal frequency, and half above. We find the lowest frequency as that which has spectral energy not greater than 0.1 percent of the maximum spectral energy,

$$S(\omega_{\min}) \le \frac{S(\omega_0)}{1000.} \tag{23}$$

Then we determine geometric spacing for N_1 points from $\omega_{\min}$ to ω_0 as follows:

$$\delta = 1.25 \tag{24}$$

$$\omega_1 = \omega_{\min} \tag{25}$$

$$\Delta\omega_i = \frac{\omega_0 - \omega_{\min}}{\frac{\delta^{n_1}-1}{\delta-1} - 0.5(1+\delta^{n-1})} \tag{26}$$

The "central" frequencies are then

$$\omega_i = \omega_{i-1} + 0.5 * \Delta\omega_{i+\Delta\omega_{i-1}} \qquad \text{for} \quad i = 2 \text{ to } N_1 \tag{27}$$

We distribute $N_2 = N - N_1$ frequencies above ω_0 in the same way, this time choosing a value of δ that yields:

$$S(\omega_{\max}) \leq \frac{S(\omega_0)}{1000.} \tag{28}$$

Then the amplitudes of the N waves representing the spectrum are found as

$$\zeta_i = \sqrt{2S(\omega_i)\Delta\omega_i} \tag{29}$$

The phases are found using a uniform random distribution from π to $-\pi$.

2.4 Simple PID Rudder Control Algorithm in LAMP

When a ship is operating in oblique seas, it is necessary to have rudder control to keep the ship on course. This is routine in model tank experiments. In the current version of the LAMP code, a simple PID (Proportional, Integral, and Derivative) control algorithm in added for course-keeping during ship motion simulation. Based on the current and desired heading angles of the ship, the following rudder command is given:

$$\delta_c = G_a(\psi - \psi_d) + G_b \frac{(\psi - \psi_0)}{\Delta t} \tag{30}$$

where

δ_c = rudder command
ψ = ship heading at the current time step
ψ_0 = ship heading at the previous time step
ψ_d = desired ship heading
G_a = gain coefficient for the proportional term
G_b = gain coefficient for the derivative term
Δt = time step size.

Only proportional and derivative terms are used. The integral term that is usually used to correct certain biases is not included in this formulation. In the current control algorithm, G_a is set to be 0.9 and G_b is set to be 20.0.

For rudder dynamics, it is assumed that the rudder servo is a linear first order lag with given slew rate R_m and proportional band P_B. Thus,

$$\tau\dot{\delta} + \delta = \delta_c \tag{31}$$

where $\tau = P_B / R_m$. In the current algorithm, P_B is set to be 5 degrees and R_m is set to be 5.5 degrees/second. If the rudder command δ_c is constant in the time interval Δt, the exact solution of equation is

$$\delta = \delta_0 + (1 - e^{-\frac{\Delta t}{\tau}})(\delta_c - \delta_0) \tag{32}$$

where δ_0 is the rudder angle at the beginning of the time step and the second term is the increment of the rudder angle. Note that this increment is limited by the rudder slew rate R_m, *i.e.*

$$\left| \frac{(1 - e^{-\frac{\Delta t}{\tau}})(\delta_c - \delta_0)}{\Delta t} \right| \le R_m \tag{33}$$

The rudder angle is limited by the maximum rudder angle A_m, *i.e.*

$$|\delta| \le A_m \tag{34}$$

In the current control algorithm, A_m is set to be 35 degrees.

2.5 A Multi-Level System

A complete computational capability for the assessment of ship motions and wave loads must be based on a multi-level approach. Such a system integrates methods that are based not just on one single code or one single level of sophistication, but rather on a system of codes with different levels of sophistication. As a general rule, the physics underlying the ship/wave interactions is best understood using comparisons generated by incremental increases in complexity - a procedure that also moderates computer usage. Analysis tools at the lower levels may employ several approximations to attain a short enough turnaround time for use in early stages of the evaluation process. Examination of results obtained by the lower level code guides the engineer in choosing areas where more accurate theories must be used. In other words, the lower level codes should be used as a filtering mechanism for the selection of more accurate but more complicated and computationally intensive codes.

A multi-level system can also effectively tie the probabilistic and deterministic approaches together providing the missing ingredient of probabilistic prediction. Statistical data of ship motion in given random seas can be obtained by using lower level evaluation codes to efficiently compute the ships responses to a very wide range of deterministic excitations. The severe ship responses can be selected from these, to be examined with the higher level nonlinear simulations. Conversely, nonlinear dynamic simulations of ships in episodic wave events can be used to understand the actual physical mechanisms underlying the ship responses to these events, such as capsizing, and to identify dominant factors of vessel stability, which can be used in the statistical screening process using the lower level codes.

Recognizing these needs, the LAMP System is being developed as a multi-level code system consisting of a total of three computational methods of different levels of sophistication.

- LAMP-4: The large-amplitude 3-D nonlinear method
- LAMP-2: The approximate large-amplitude 3-D nonlinear method
- LAMP-1: The linearized 3-D time-domain method

The LAMP-4 method is the complete large-amplitude method where the 3-D potential is computed with the linearized free-surface condition satisfied on the surface of the incident wave. Both the hydrodynamic and hydrostatic pressures are computed over the instantaneous hull surface below the incident wave surface. Large computer resources are required for this method. In the LAMP-2 method, the linear 3-D approach is used to compute the hydrodynamic part of the pressure forces, while the hydrostatic restoring and Froude-Krylov forces are calculated with the same accuracy as in LAMP-4. The reason for developing this simplified method is that it drastically reduces the requirements for computer resources. The LAMP-1 method is the linearized version of the LAMP-4 method. This 3-D time-domain method includes a routine for automatic generation of the frequency domain results.

Table 2 shows how the hydrostatic restoring and Froude-Krylov forces and the hydrodynamic (added mass, damping and diffraction) forces are calculated for the four different LAMP methods. The hardware requirements for the four methods are also shown in Table 2. Note that the two nonlinear methods, LAMP-2 and LAMP-4 are based on the approach that both the motions and the waves may have large amplitudes. For all of these three nonlinear methods, the restoring and Froude-Krylov forces are calculated exactly over the instantaneous wetted surface below the incoming wave surface.

Table 2. Computation Methods and Hardware Requirements for the LAMP Code

(Z=0 and F(t) are Still Water Surface and Incident Wave Surface, Respectively)

Method	**Hydrodynamic, Restoring, and Froude-Krylov Forces**	**Hardware**
LAMP-4	Free Surface Boundary Conditions on F(t) 3-D Large-Amplitude Hydrodynamics Nonlinear Restoring and Froude-Krylov Forces	Fast Workstation
LAMP-2	Free Surface Boundary Conditions on F(t) 3-D Linear Hydrodynamics Nonlinear Restoring and Froude-Krylov Forces	Workstation
LAMP-1	Free Surface Boundary Conditions on Z=0 3-D Linear Hydrodynamics Linear Restoring and Froude-Krylov Forces	Workstation

3 Fishing Vessel Model and Static Stability

3.1 Model for LAMP

Figure 3 shows a body plan view of the fishing vessel *Italian Gold* , as it was designed. As noted in the Coast Guard Report (USCG, 1994), these plans do not correspond exactly to the vessel as built. These design drawings are the best available model of the hull, and were used by the Coast Guard in their analysis.

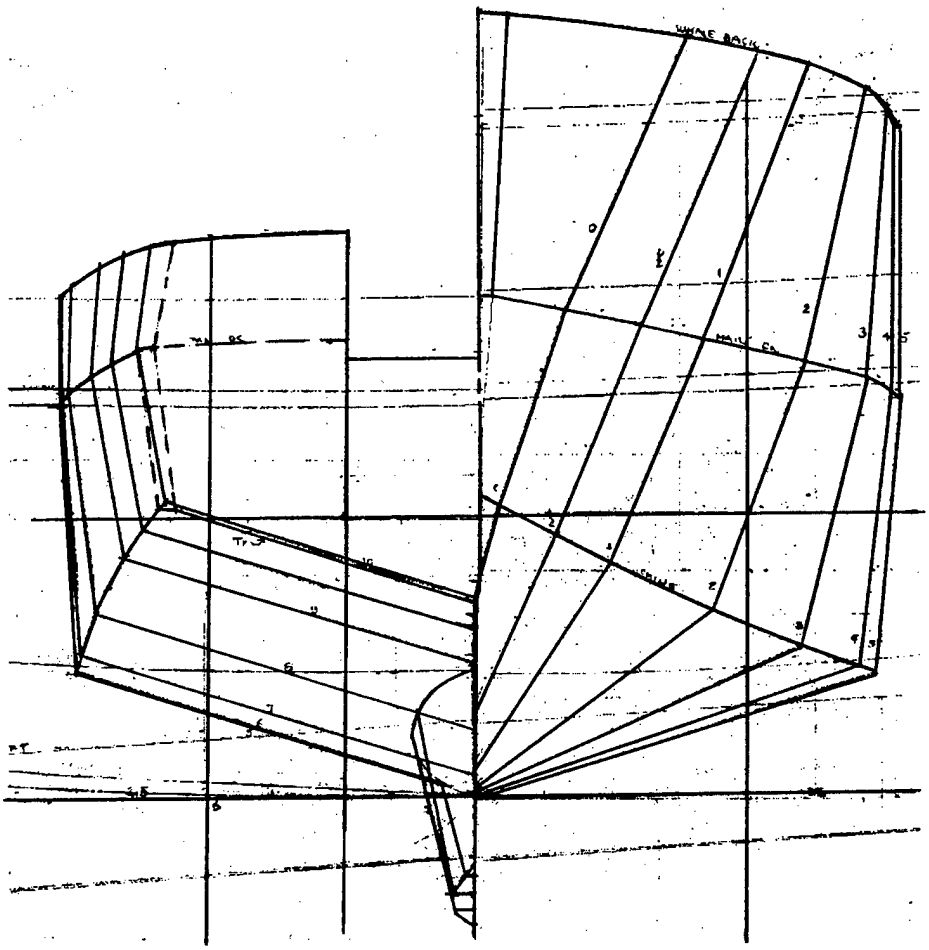

Figure 3. Body Plan of the Fishing Vessel

The LAMP program requires a full surface definition, represented by an array of quadrilateral panels. This geometry was created by measuring the ship's molded keel line, chine line, and main and whaleback deck lines. A reasonable approximation to the developable surface was obtained by distributing points along each of these lines in proportion to arc length. Figure 4 shows this panelization in a body plan view. The left side shows the original panelization. In order to reduce the number of surfaces for the LAMP calculation, the chine was "softened," so that the lower hull and the upper hull could be joined as one surface without a hard line. This geometry is shown on the right side of Figure 4. A profile view of the "softened" geometry is shown in Figure 5.

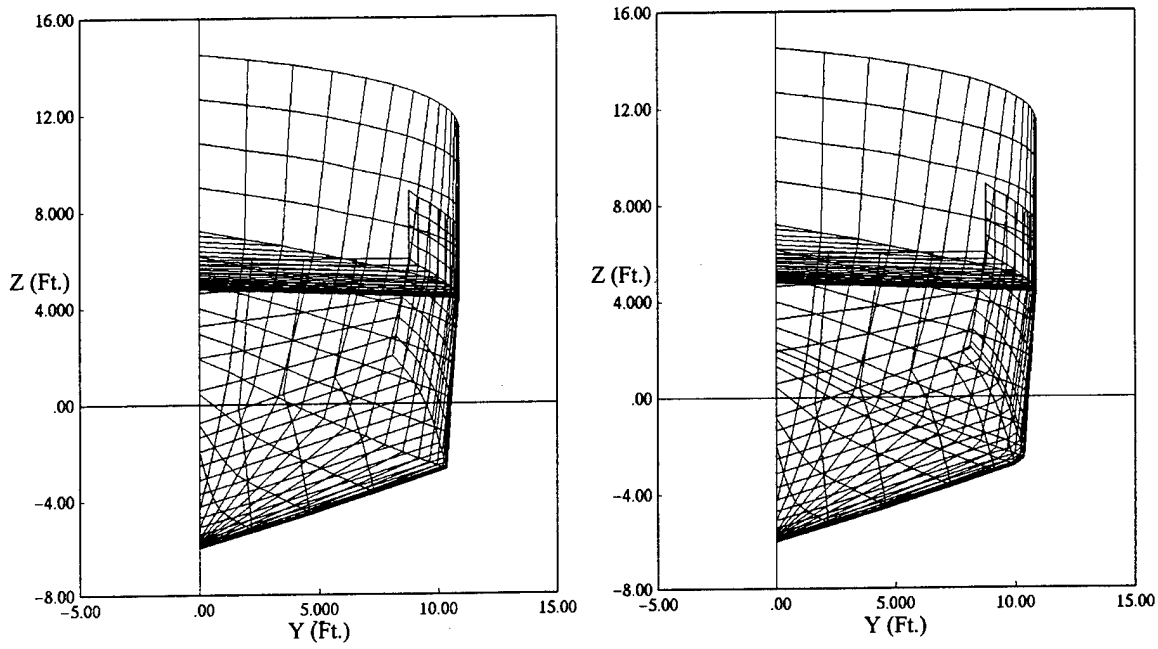

Figure 4. Original and Softened Panelization - Body Plan

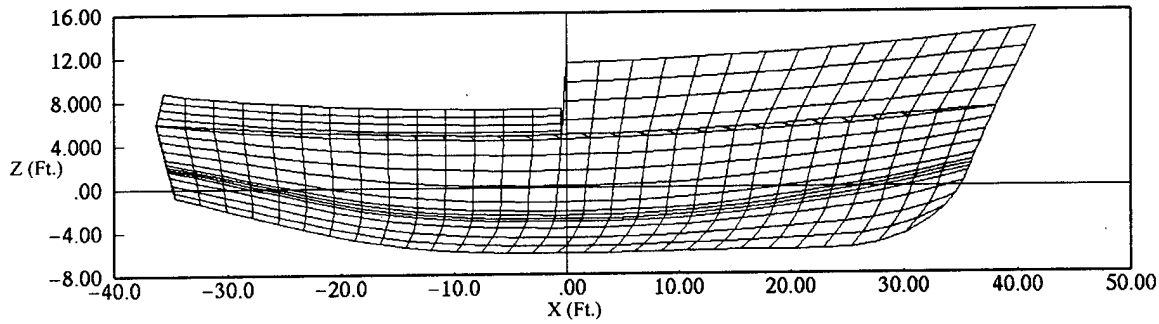

Figure 5. Profile View of Softened Panelization

3.2 Hydrostatic Stability

An evaluation of the undamaged hydrostatic stability of the vessel was performed using LAMP hydrostatics and data from the Coast Guard Report on the casualty (USCG, 1994). This report evaluated the vessel in its designed configuration, not "as-built". The design drawings (Gilbert Associates, 1979) were used for the USCG geometry as well as the LAMP geometry for an assumed loading condition as follows:

Loading Condition	English Units	Metric Units
Displacement	190.73 LT	193.79 MT
VCG above Baseline	8.87 ft	2.70 m
LCG Relative to Amidships	2.77 ft Aft	0.88 m

The LAMP hydrodynamic model did not include the skeg, the rabbet, the propeller, the rudder and other appendages. These appendages were included as components generating viscous, but not hydrodynamic forces. The hydrostatics generated by LAMP reflect these differences. The intent of the LAMP hydrostatic calculations was to establish the static stability of the vessel as seen by LAMP for our calculation. When applying the displacement of 190.73 Long Tons (193.79 MT), the LAMP hydrostatics gave a baseline draft amidships of 8.422 ft (2.567 m), deeper than the USCG draft. The USCG report did not provide the draft at zero heel and trim for the undamaged condition, but the baseline draft for heel angle of 3.89 degrees was given as 7.827 ft (2.386 m). We chose to match the displacement rather than the draft.

LAMP was used to generate the vessel's righting arm or GZ curve versus heel angle. The vessel is given a fixed heel angle and lowered into the water. When the vertical buoyancy force matches the displacement, the transverse moment about the center of gravity is measured. This quantity is divided by the displacement to give the righting arm.

In Figure 6, the LAMP GZ curve is plotted along with the wind-heeling arm from the USCG calculations. The wind force is based on a 53.4 knot steady wind abeam. It takes into account the components of the above-water structure. The first intersection of these curves shows the static heel angle that would be produced by this wind abeam, approximately 6 degrees. The second intersection shows the maximum angle due to wave action that can be sustained before capsize in this wind, approximately 46 degrees. This analysis assumes a calm free surface, while the actual hydrostatic stability in a seaway will depend on the actual wave elevation.

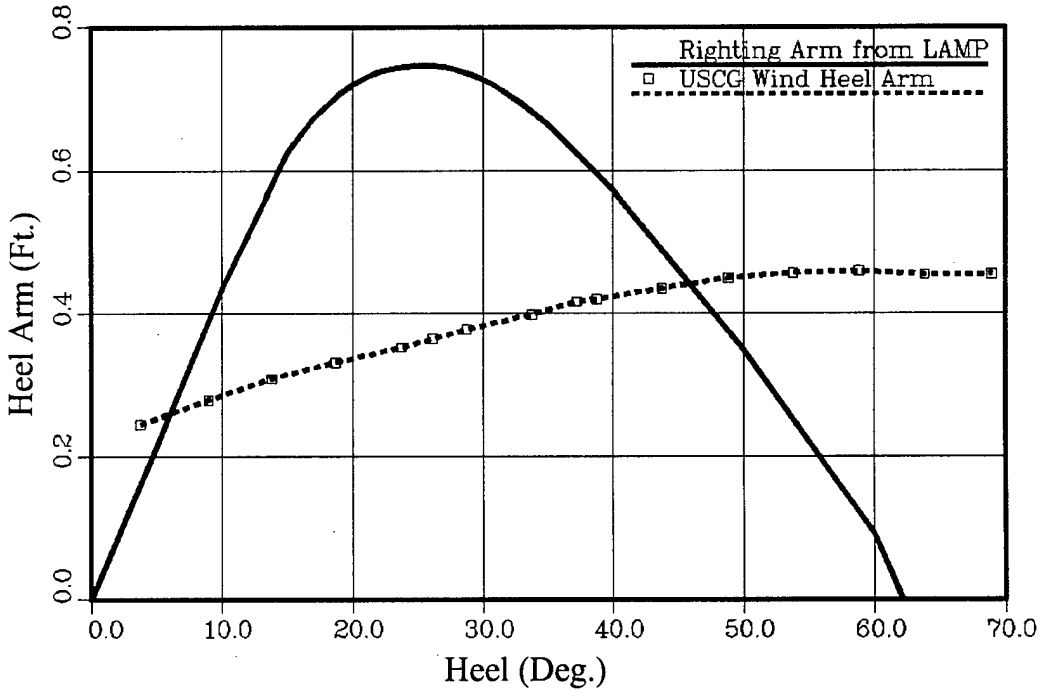

Figure 6. Static Stability of Fishing Vessel with USCG Wind Heel

4 Nonlinear Motion Simulation of Fishing Vessel in Stern Quartering Seas

To demonstrate the application of the improved LAMP code for assessing the dynamic stability of a fishing vessel in waves, a series of computations were performed using LAMP-2 for the *Italian Gold* in regular and irregular stern quartering waves. Only intact stability is studied. The center of gravity, CG, of the ship is located amidship and is about 0.27 ft (82.29 cm) above the design waterline in the current study. The actual location of the center of gravity depends on the weight distribution of the ship and is a very important factor in the roll stability. The CG used in the current calculations is a reasonable one for such a fishing vessel in full load condition.

In principle, the LAMP code is applicable to general large-amplitude motion simulation, including capsizing, of ships in a wide range of sea conditions. For the current study, uni-directional linear incident waves are selected. The wave conditions for the runs with regular incident waves are listed in Table 3 and for the runs with irregular incident waves represented by Pierson-Moskowitz spectrum are listed in Table 4. Note that ω is the wave frequency, λ is the wavelength, h is the wave height, $h_{1/3}$ is the significant wave height, and L is the ship length (68 ft, 20.7 m). The wave amplitude and wave frequency are varied to see the effects of these parameters on capsizing. All waves selected are bounded by the "steepest wave" limit.

Table 3. Regular Wave Cases of LAMP Runs

Case No.	ω (rad/sec)	λ (ft)	H (ft)	λ (m)	h (m)	h/L	h/λ
R-1	1.7000	70	6	21.3	1.8	0.088	0.086
R-2	1.4224	100	6	30.5	1.8	0.088	0.060
R-3	1.2021	140	6	42.7	1.8	0.088	0.043
R-4	0.8500	280	6	85.3	1.8	0.088	0.021

Table 4. Random Wave Cases of LAMP Runs

One Parameter Pierson-Moskowitz Spectrum

Case No.	$h_{1/3}$ (ft)	$h_{1/3}$ (m)
IR-1	10	3.1
IR-2	13	4.0
IR-3	15	4.6

As for the ship operating condition, the forward speed is set to be 10 knots; the initial roll, pitch, and yaw angles are zero; and the ship is at the bottom of the incident wave. The incident wave is coming from the starboard direction of the stern. The angle between the direction of the wave propagation and the direction of the ship forward motion is 45 degrees. In all simulation runs, a

PID control is used for course-keeping purpose. Six-degree-of-freedom coupled equations of motions are solved at each time step for motion simulation.

A sequence of snap shots for case R-2 (λ=100 ft, 30.5 m) is given in Figure 7. These snap shots are approximately one second apart during a 10-second simulation run. The ship started on course and the bow was pushed toward the port side by the stern quartering wave coming from the starboard. The autopilot system tried to maintain the original course by turning rudder toward the port side. As can be seen in the picture, the ship bow was turning back and at the same time rolling toward the port side. The second wave crest hit the ship from the starboard at the time it was rolling toward the port side. As a result, the ship capsized due to dynamic effect. This is a typical broaching phenomenon. The behavior of the ship is closely related to the wave characteristics.

Plots of the motion histories in six directions and snap shots for the plotted case are given from Figure 8 to Figure 11. In these figures, the dimension for linear displacement is ft and the dimension for the rotation is degrees. Notice that when the wavelength is about 1 to 2 ship lengths, the ship will capsize even though the wave height is only 6 ft (1.8 m). When the wavelength is four times the ship length (case R-4, Figure 11), the ship is just riding on the wave and does not capsize.

Numerical simulations have also been done for *Italian Gold* in fully developed random seas. The motion histories for three cases (IR-1 with $h_{1/3}$=10 ft (3.1 m), IR-2 with $h_{1/3}$=13 ft (4.0 m), and IR-3 with $h_{1/3}$=15 ft (4.6 m) are shown in Figure 12 to Figure 14. It can be seen clearly that the ship capsized while the significant wave height reached 13 ft (4.0 m). It is interesting to see that the ship can survive in 10 ft (3.1 m) random sea but will capsize in 6 ft (1.8 m) regular sea. It also indicates that the most dangerous condition in a random sea is when several waves group together like a regular sea condition.

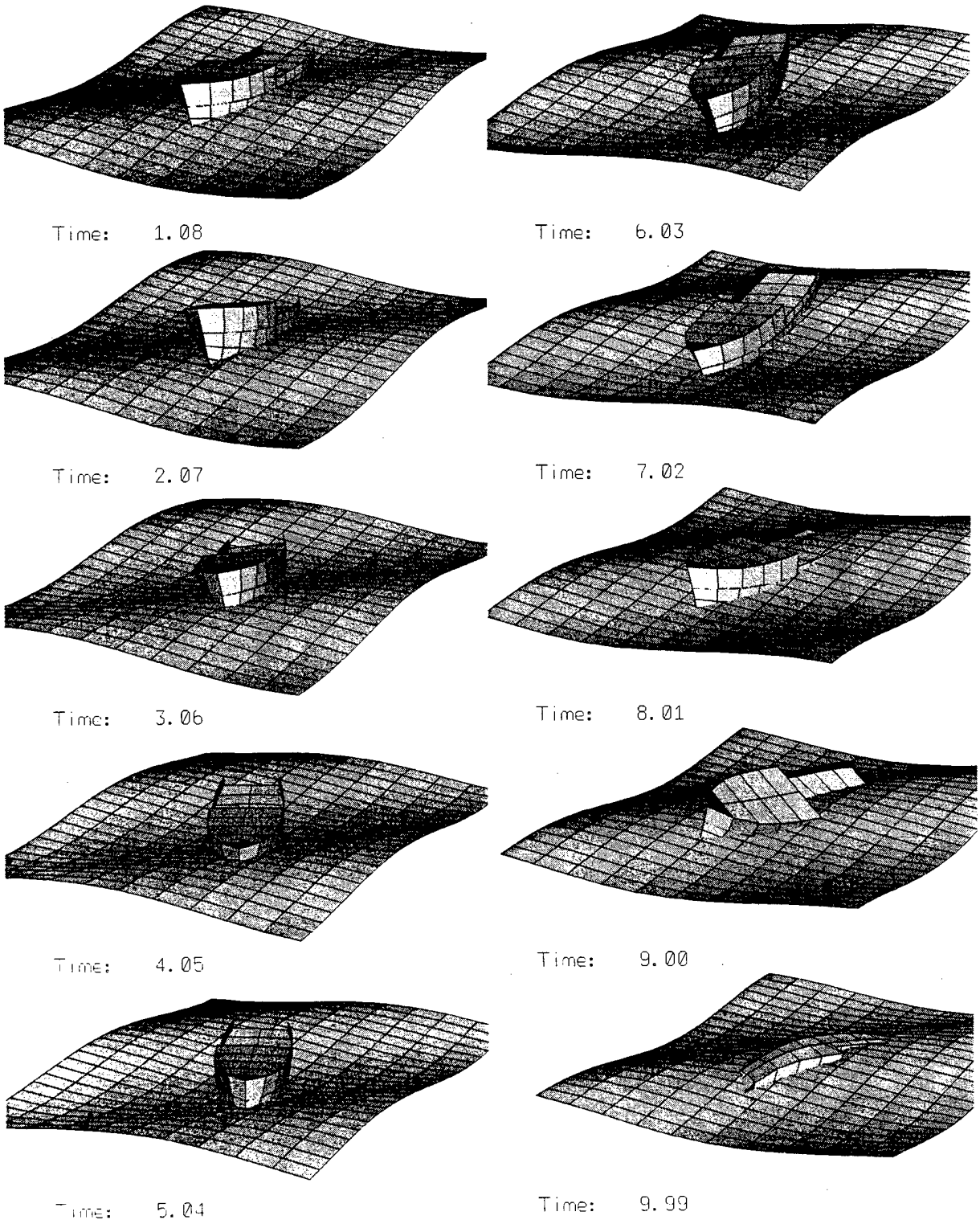

Figure 7. Case R-2: Snap Shots of Motion Animation of Fishing Vessel *Italian Gold* in Linear Regular Stern Quartering Waves with λ=100 ft (30.5 m)

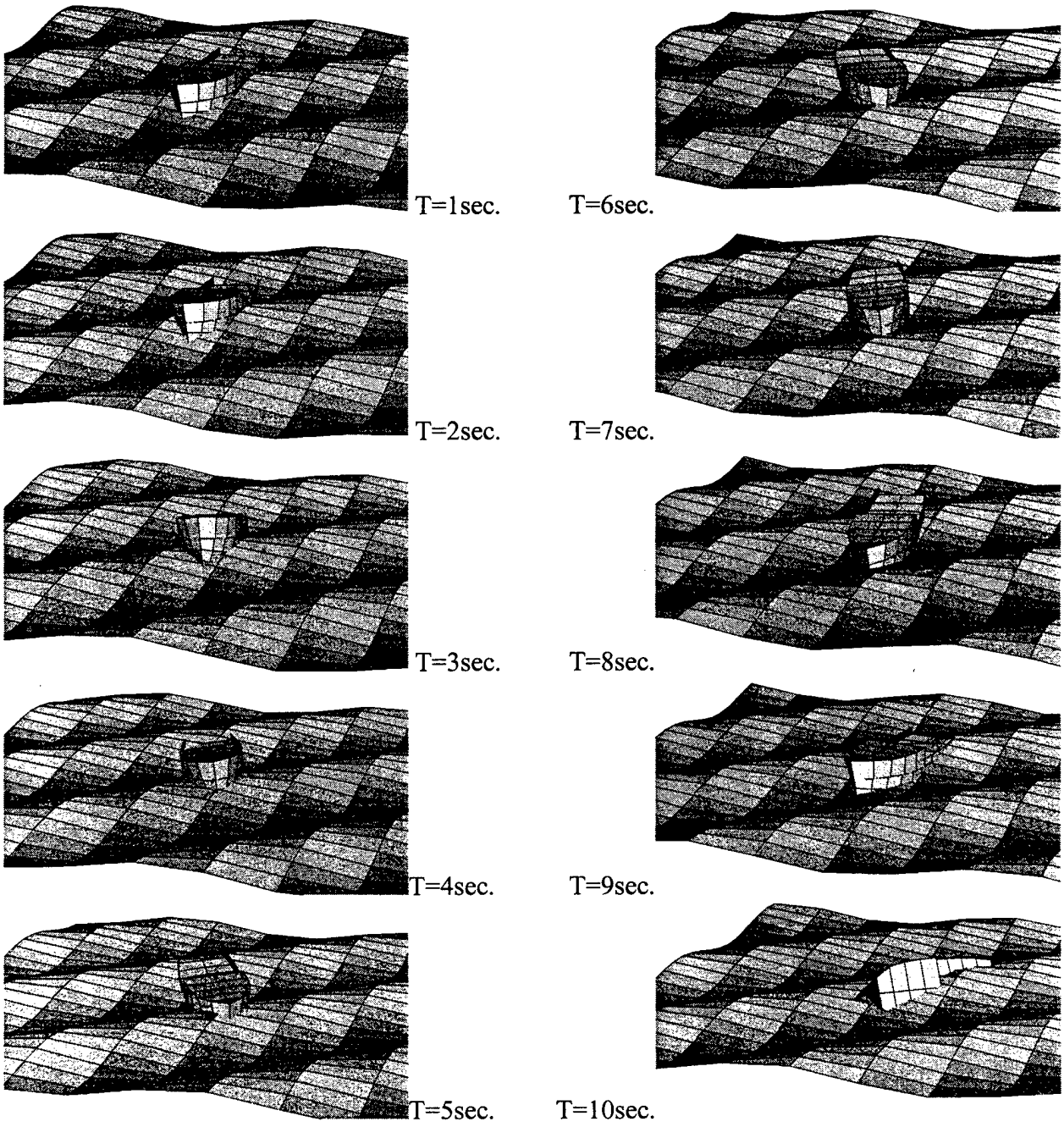

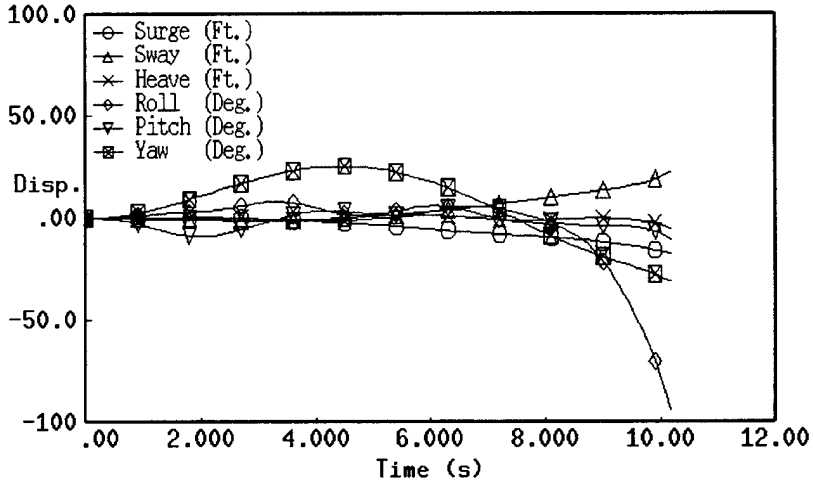

Figure 8. Case R-1: Time History of Motions in Six Directions for Fishing Vessel *Italian Gold* in Linear Regular Stern Quartering Waves with λ=70 ft (21.3 m)

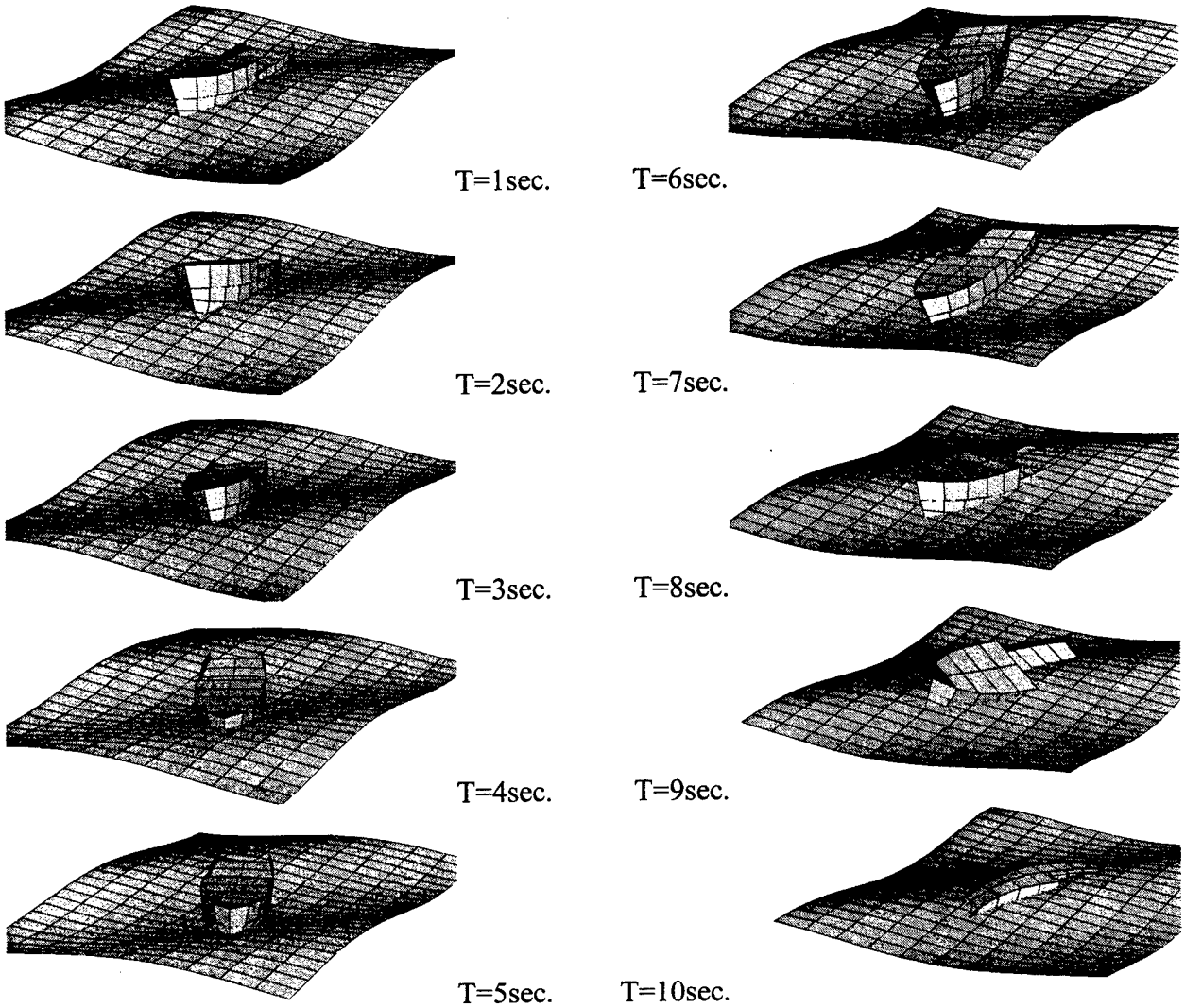

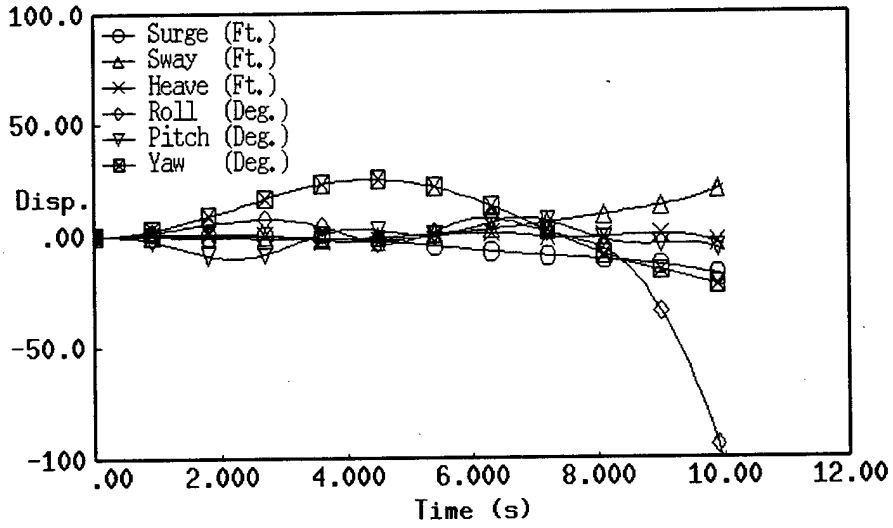

Figure 9. Case R-2: Time History of Motions in Six Directions for Fishing Vessel *Italian Gold* in Linear Regular Stern Quartering Waves with λ=100 ft (30.5 m)

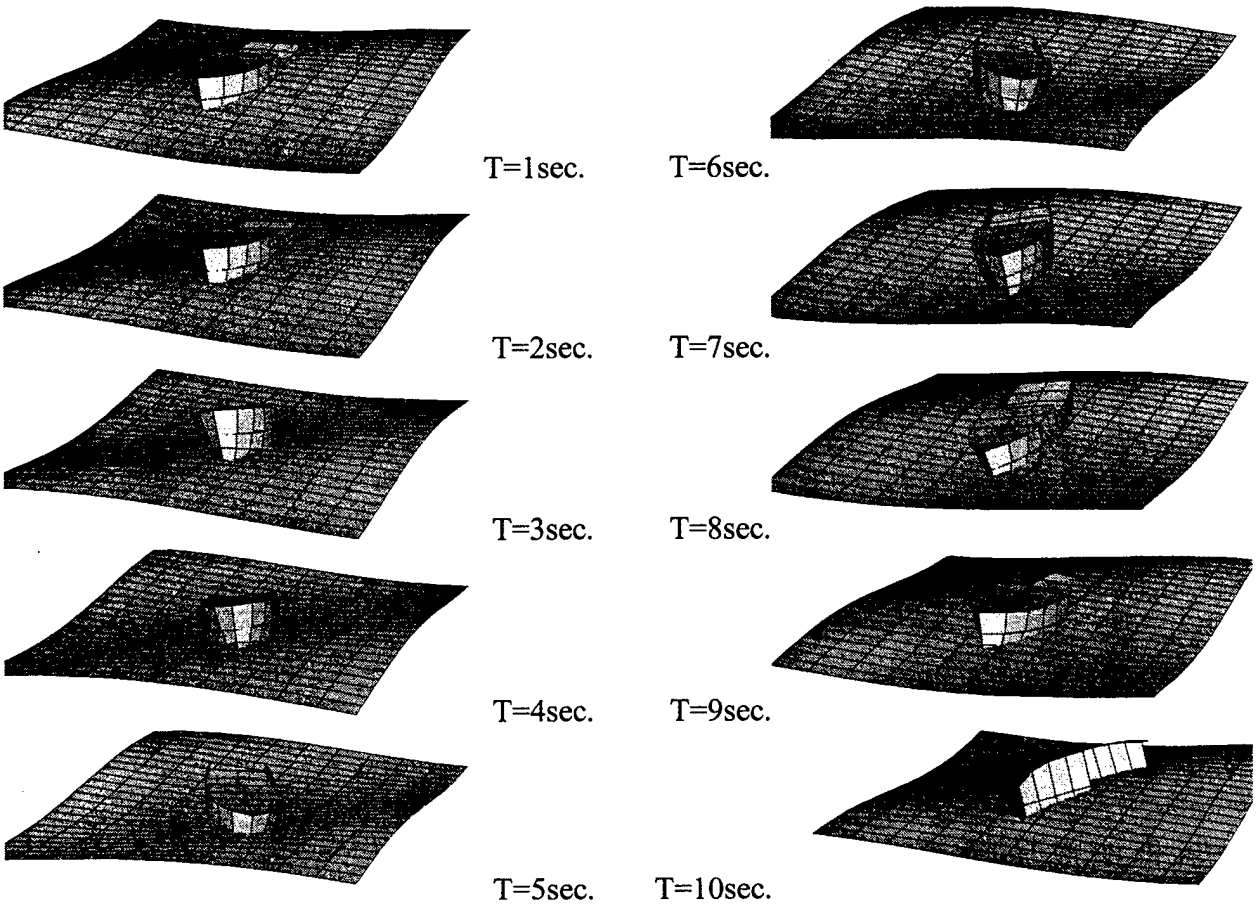

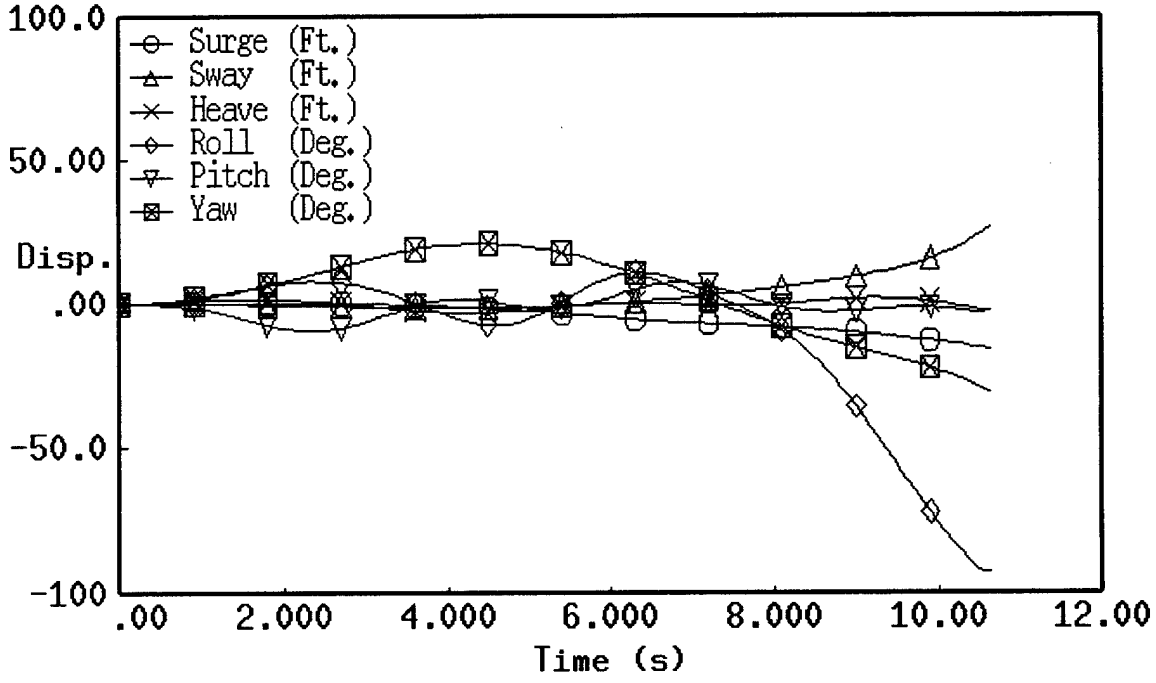

Figure 10. Case R-3: Time History of Motions in Six Directions for Fishing Vessel *Italian Gold* in Linear Regular Stern Quartering Waves with λ=140 ft (42.7 m)

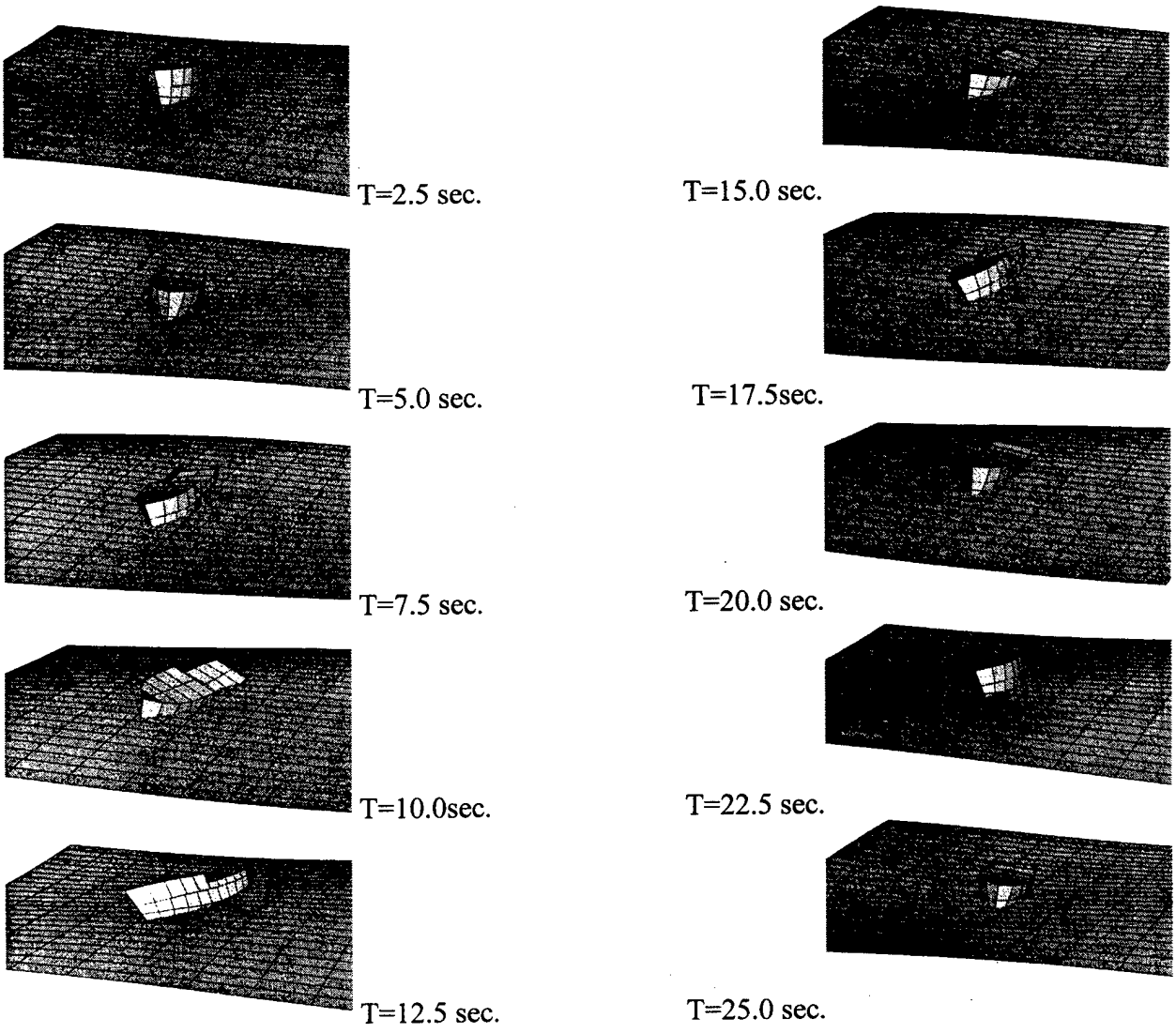

Figure 11. Case R-4: Time History of Motions in Six Directions for Fishing Vessel *Italian Gold* in Linear Regular Stern Quartering Waves with λ=280 ft (85.3 m)

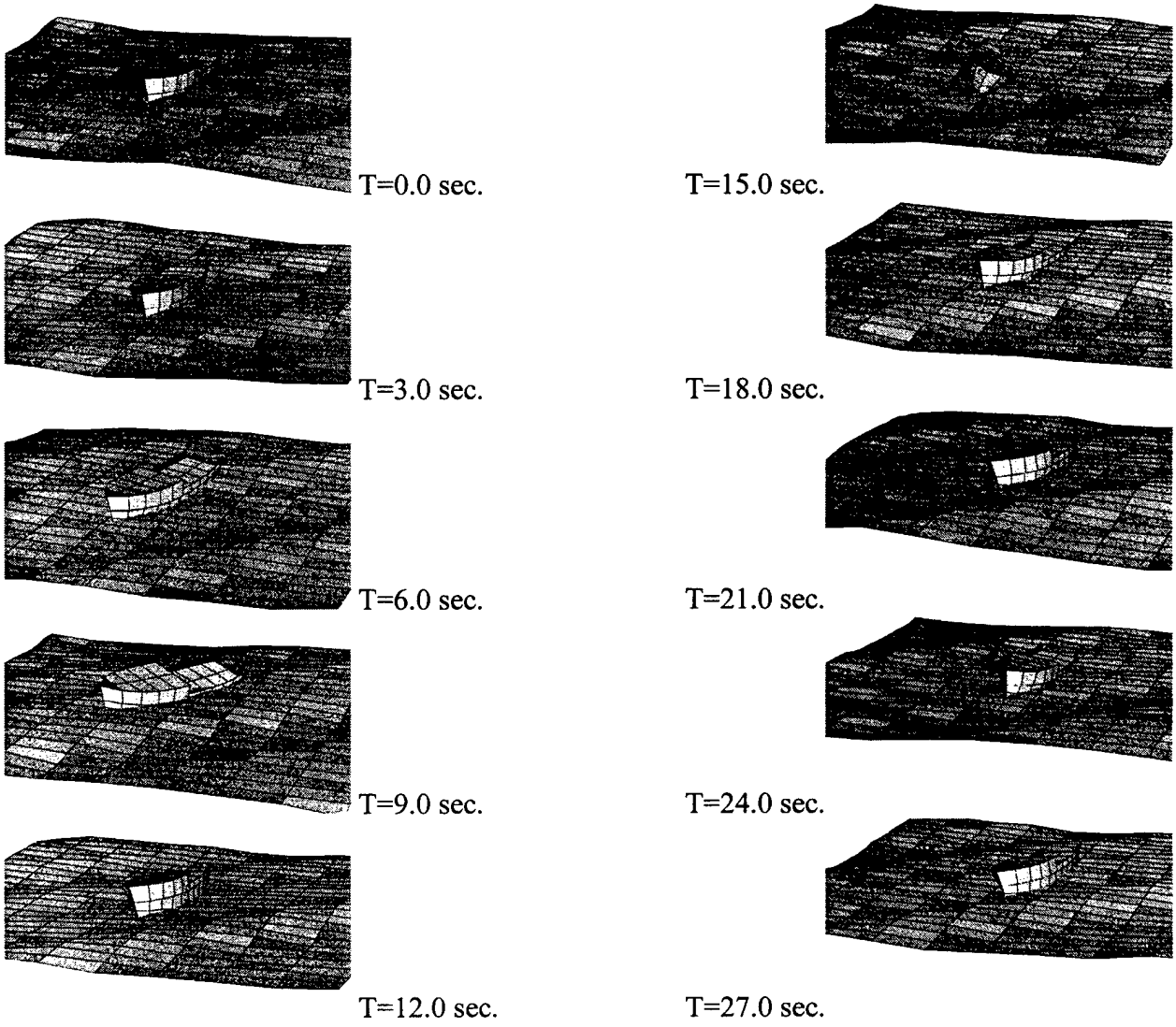

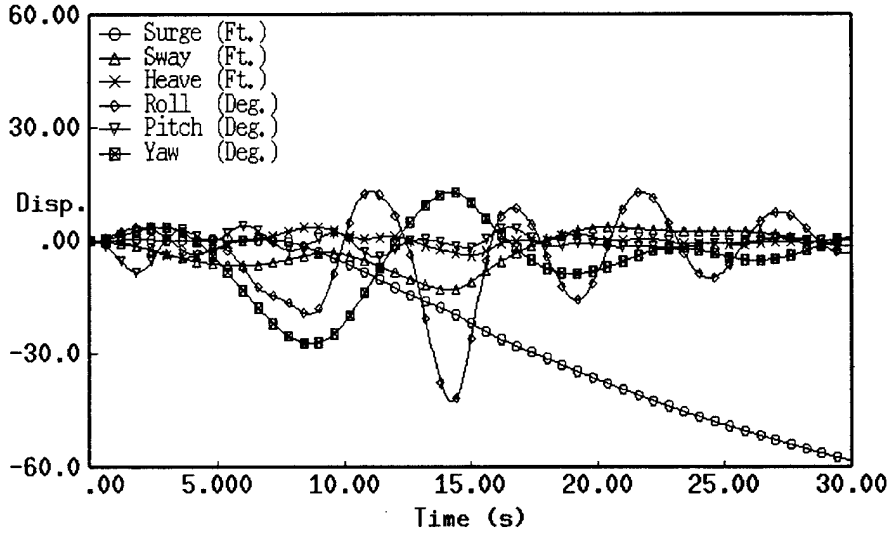

Figure 12. Case IR-1: Time History of Motions in Six Directions for Fishing Vessel *Italian Gold* in Linear Random Stern Quartering Waves with $h_{1/3}$=10 ft (3.0 m)

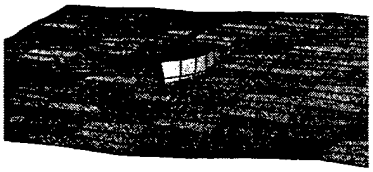

T=0.0 sec.

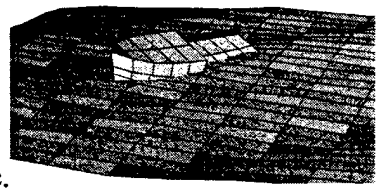

T=8.55 sec.

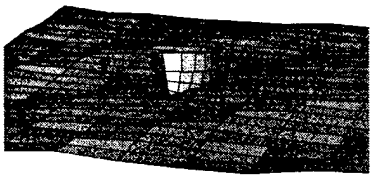

T=1.71 sec.

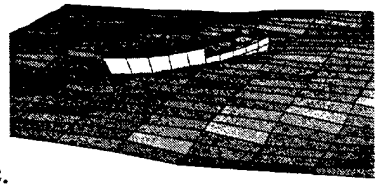

T=10.26 sec.

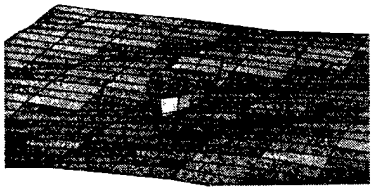

T=3.42 sec.

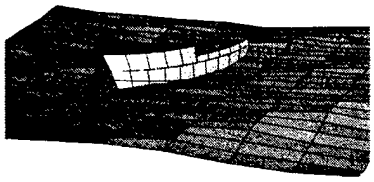

T=11.97 sec.

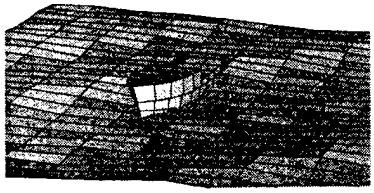

T=5.13 sec.

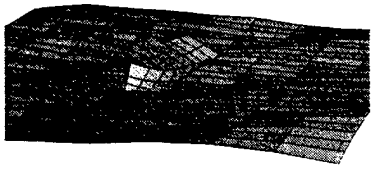

T=13.68 sec.

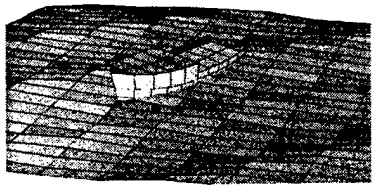

T=6.84 sec.

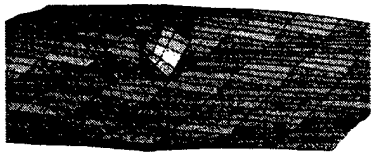

T=15.39 sec.

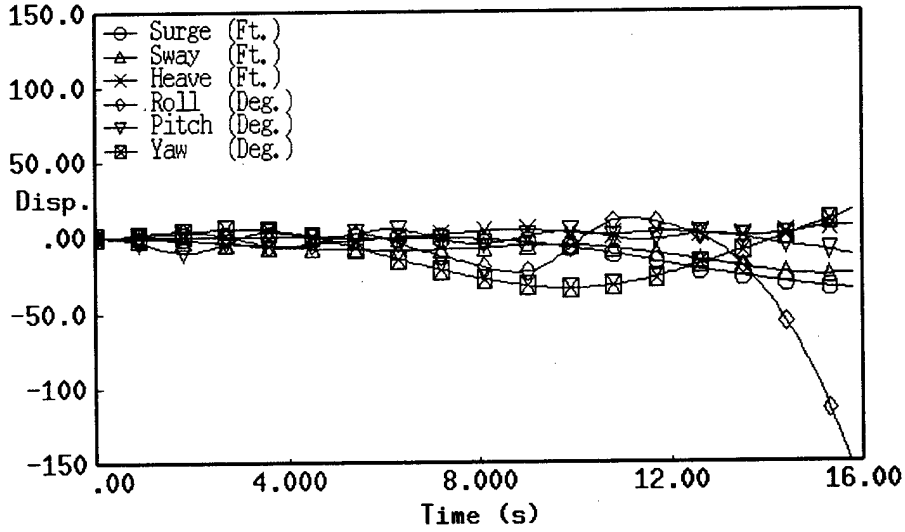

Figure 13. Case IR-2: Time History of Motions in Six Directions for Fishing Vessel *Italian Gold* in Linear Random Stern Quartering Waves with $h_{1/3}$=13 ft (4.0 m)

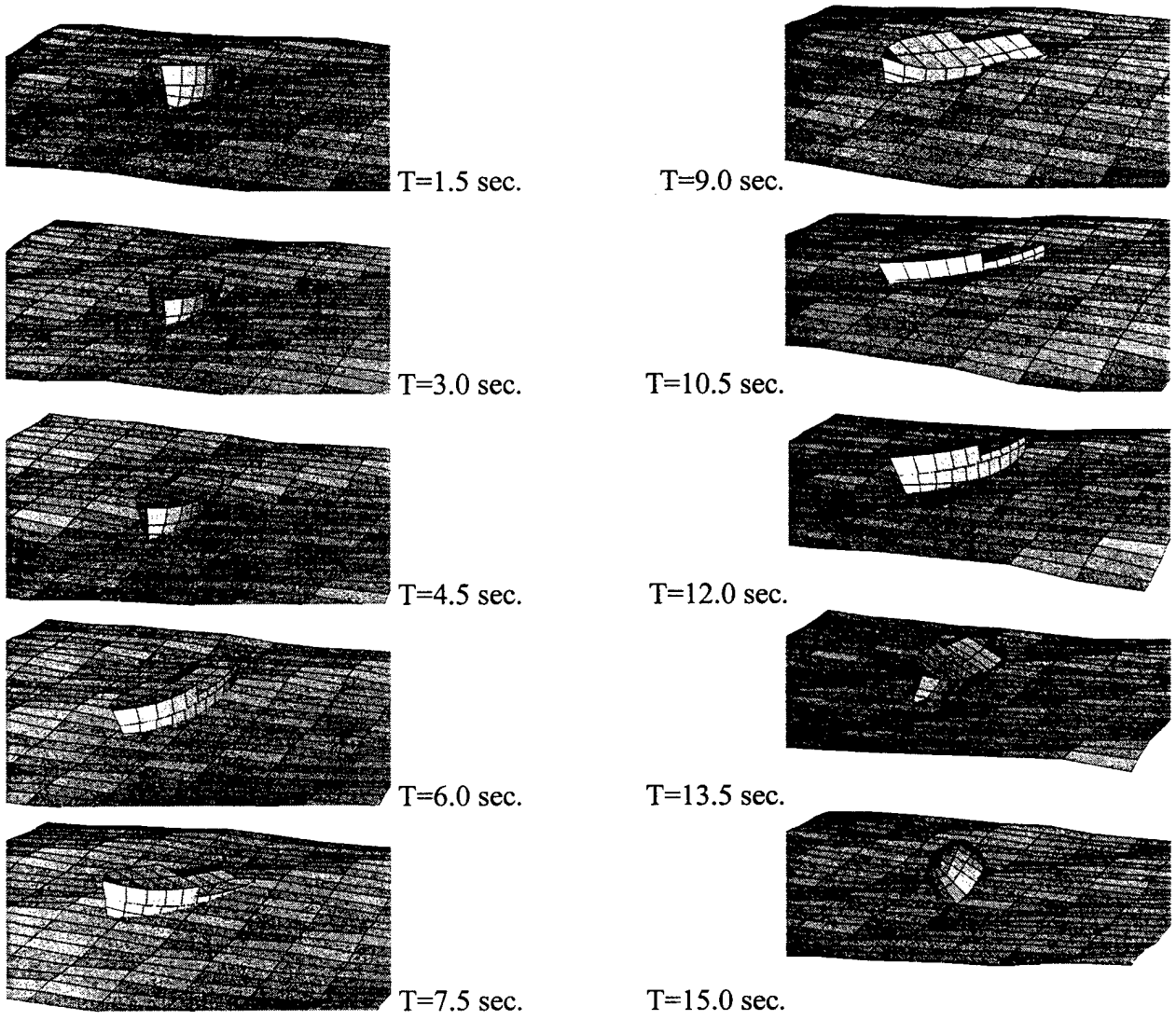

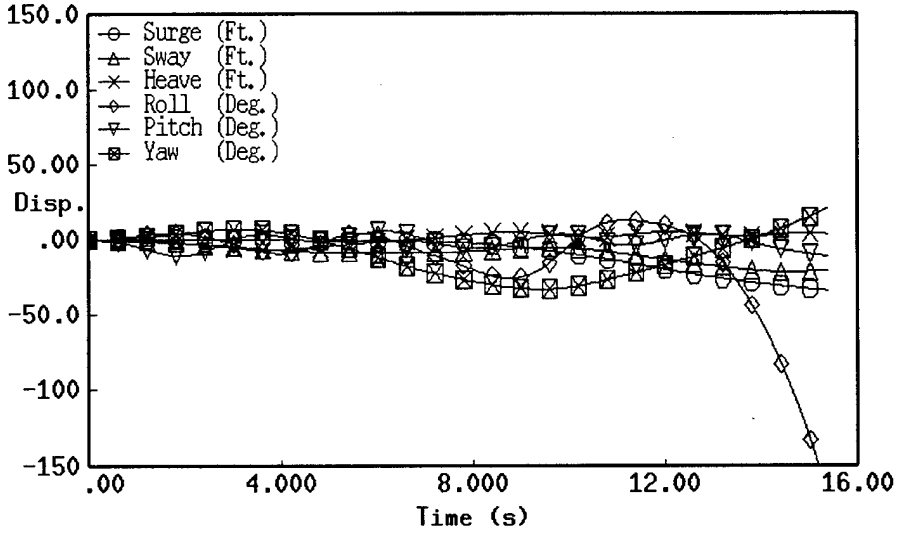

Figure 14. Case IR-3: Time History of Motions in Six Directions for Fishing Vessel *Italian Gold* in Linear Random Stern Quartering Waves with $h_{1/3}$=15 ft (4.6 m)

5 Summary

A new numerical simulation method, LAMP, has been developed for studying the extreme motion including capsizing of ships in oblique seas. A sample study of the static and dynamic stability of a typical fishing vessel *Italian Gold* is presented in this report. LAMP motion simulations of the ship in various incident waves were performed. It was found that under the specified loading condition, the ship will capsize in stern quartering sea condition while the wavelength is about 1 to 2 times the ship length and wave height is 6 ft (1.8 m).

On the other hand, the ship is able to survive 10 ft (3.0 m) significant wave height in a fully developed random sea. However, the condition reported at the time while *Italian Gold* capsized was 55 knots NE wind. This corresponds to sea state 7 with significant wave height of 19 ft (5.8 m). As shown in the numerical simulation, the ship would not be able to survive at the given loading condition.

Only intact stability was considered in this study. From the numerical results, it is found that water on deck may be important for ships in several different wave conditions. Loads due to water on deck or possible compartment flooding should be taken into consideration in the future study. Wind force may be another important factor. Wind force will create steady heeling moment, which will further reduce the stability. Both of these factors are unfavorable to the stability of the ship.

The current LAMP simulation is full six-degree-of-freedom with speed condition. Although viscous and lifting effects are included (skin friction, bilge keel and rudder). Several other important factors, such as the propeller thrust, the effect of the propeller slipstream on the rudder, the effect of boundary layer separation at the stern of the vessel on the maneuvering characteristics of the vessel, wind effects, and nonlinear wave effects, were not modeled in this simulation and should be included in any future studies.

6 References

Alman, P., Cleary, W.A. Jr., Dyer, M.G., Paulling, J.R., and Salvesen, N. (1992), "The International Load Line Convention: Crossroad to the Future," Marine Technology, Vol. 29, No. 4.

Beck, R.F., and Magee, A. (1991), "Time-Domain Analysis for Predicting Ship Motions," Developments in Marine Technology: 7: Dynamics of Marine Vehicles and Structures in Waves, Elsevier Science Publishers B.V., Amsterdam.

Bingham, H.B., Korsmeyer, F.T., Newman, J.N., and Osbone, G.E. (1993), "The Simulation of Ship Motions," Proceedings of the 6th International Conference on Numerical Ship Hydrodynamics, Iowa City, Iowa.

Cao, Y., Lee, T., and Beck, R.F. (1992), "Computation of Nonlinear Waves Generated by Floating Bodies," Proceedings of the 7th International Workshop on Water Waves and Floating Bodies, Val de Reuil, France.

de Kat, J.O., and Paulling, J.R. (1989), "The Simulation of Ship Motions and Capsizing in Severe Seas," Transactions of the Society of Naval Architects and Marine Engineers, 97.

Dillon, E.S., Ebel, F.G., and Goobeck, A.R. (1962), "Ship Design for Improved Cargo Handling," Transactions of the Society of Naval Architects and Marine Engineers, Vol. 70, 1962.

Sarchin, T.H., and Goldberg, L.L. (1962), "Stability and Buoyancy Criteria for U.S. Naval Surface Ships," Transactions of the Society of Naval Architects and Marine Engineers, Vol. 70, 1962.

Frank, W., and Salvesen, N. (1970), "The Frank Close-Fit Ship Motion Computer Program," DTNSRDC, Report 3289.

Fujino, M., and Yoon, B.S. (1986), "A Practical Method of Estimating Ship Motions and Wave Loads in Large Amplitude Waves," International Shipbuilding Progress, 33.

Grove, T.W., Rynn, P.G., and Ashe, G.M. (1992), "Bulk Carriers, A Cause for Concern," presented at the June 4, 1992, Meeting of the Great Lakes/Great Rivers Section of The Society of Naval Architects and Marine Engineers.

Gilbert and Assoc. (1974), Lines of Stern Dragger, Drawing D-171-1.

Gilbert and Assoc. (1974), Outboard Profile of Stern Dragger, Drawing D-171-2.

Gilbert and Assoc. (1979), General Arrangement of Stern Dragger, Drawing D-171-3.

Gilbert and Assoc. (1979), Inboard Profile of Stern Dragger, Drawing D-171-4.

Himeno, Y. (1981), "Prediction of Ship Roll Damping - State of the Art", Department of Naval Architecture and Marine Engineering, University of Michigan, Ann Arbor, Michigan.

Hoerner, S.F. (1951), *Aerodynamic Drag*, published by the author.

Holden, K.O., Faltinsen, O., and Moan, T., editors (1991), FAST '91, Proceedings from the First International Conference on Fast Sea Transportation, Trondheim, Norway, June 1991.

Ikeda, Y., Himeno, Y., and Tanaka, N. (1978), "Components of Roll Damping of Ship at Forward Speed," Journal of the Society of Naval Architects of Japan, Vol. 143.

Kato, H. (1958), "On the Frictional Resistance to the Roll of Ships," Journal of the Society of Naval Architects of Japan, Vol. 102.

Kato, H. (1966), "Effect of Bilge Keels on the Rolling of Ships," Memories of the Defense Academy, Japan, Vol. 4.

Kennel, C., White, B.L., and Comstock, E. N. (1985), "Innovative Designs for North Atlantic Operations," Transactions of the Society of Naval Architects and Marine Engineers, 93.

Kirkman, K.L., Nagle, T.J., and Salsich, J.O. (1983), "Sailing Yacht Capsizing," Proceedings of the Chesapeake Sailing Yacht Symposium, Annapolis, Maryland.

Korsmeyer, F.T., Ma, C., Xu, H., and Yue, D.K.P. (1992), "The Fully Nonlinear Diffraction of Water Waves by a Surface Piercing Strut," Proceedings of the 19th Symposium on Naval Hydrodynamics, Seoul, Korea.

Korvin-Kroukovsky, B.V. (1955), "Investigation of Ship Motions in Regular Waves," Transactions of the Society of Naval Architects and Marine Engineers, 63.

Lin, W.M., and Yue, D.K.P. (1990), "Numerical Solutions for Large-Amplitude Ship Motions in the Time-Domain," Proceedings of the 18th Symposium on Naval Hydrodynamics, The University of Michigan, Ann Arbor, MI, U.S.A.

Lin, W.M., and Meinhold, M. (1991), "Summary Technical Report of Hydrodynamics Loads Calculations for Advanced Marine Enterprises," SAIC Report No. 91-1050 (revised).

Lin, W.M., and Yue, D.K.P. (1992), "Wave Forces on A Surface-Piercing Sphere Undergoing Large-Amplitude Motions," Proceedings of the Seventh International Workshop on Water Waves and Floating Bodies, Val de Reuil, France.

Lin, W.M., Meinhold, M., and Salvesen, N. (1992), "IDEAS System for Ship Motions and Wave Loads," SAIC Report No. 92-1187.

Lin, W.M., and Yue, D.K.P. (1993), "Time-Domain Analysis for Floating bodies in Mild-Slope Waves of Large Amplitude," Proceedings of the Eighth International Workshop on Water Waves and Floating Bodies, St. John's, Newfoundland, Canada.

Lin, W.M., Meinhold, M., Salvesen, N., and Yue, D.K.P. (1994), "Large-Amplitude Motions and Waves Loads for Ship Design," Proceedings of the 20th Symposium on Naval Hydrodynamics, University of California, Santa Barbara, California, USA.

Liu, D., Spencer, J., Itoh, T., Kawachi, S., and Shigematsu, K. (1992), "Dynamic Load Approach in Tanker Design," Transactions of the Society of Naval Architects and Marine Engineers, 100.

Maskew, B. (1991), "A Nonlinear Numerical Method for Transient Wave/ Hull Problems on Arbitrary Vessels," Transactions of the Society of Naval Architects and Marine Engineers, 99.

Meyers, W.G., Applebee, T.R., and Baitis, A.E. (1981),"Users Manual for the Standard Ship Motion Program, SMP," DTNSRDC Report SPD-0936-01 .

Nakos, D.E., and Sclavounos, P.D. (1990), "Ship Motions by a Three-Dimensional Rankine Panel Method," Proceedings of the 18th Symposium on Naval Hydrodynamics, Ann Arbor, Michigan.

O'Dea, J.F., Powers, E.J., and Zseleczky, J. (1992), "Experimental Determination of Nonlinearities in Vertical Plane Ship Motions," Proceedings of the 19th Symposium on Naval Hydrodynamics, Seoul, Korea.

Ogilvie, T.F., and Tuck, E.O. (1969), "A Rational Strip-Theory of Ship Motion: Part I," Department of Naval Architecture, University of Michigan, Report No. 013.

Paik, J.K., Kim, D.H., Bong, H.S., Kim, M.S., and Han, S.K. (1992), "Deterministic and Probabilistic Safety Evaluation for A New Double-Hull Tanker With Transverseless System, Transactions of the Society of Naval Architects and Marine Engineers, 100.

Pawlowski, J.S., and Bass, D.W. (1991), "A Theoretical and Numerical Model of Ship Motions in Heavy Seas," Transactions of the Society of Naval Architects and Marine Engineers, 99.

Price, W.G., and Bishop, R.Z.D. (1977), *Probabilistic Theory of Ship Dynamics*, printed by T. A. Constable, Ltd.

Rousmaniere, J. (1980), *Fastnet, Force 10*, W.W. Norton Company.

Salvesen, N., and Lin, W.M. (1993), "SAFE SEAS - Vessel Safety Assessment for Extreme Seas - A New National Capability," Proceeding of the Vessel Stability Symposium, U.S. Coast Guard Academy, New London, Connecticut.

Shark, G., Shin, Y.S., and Spencer, J.S. (1989), "Dynamic-Response-Based Intact and Residual Damage Stability Criteria for SemiSubmersible Units," Transactions of the Society of Naval Architects and Marine Engineers, 97.

Stephens, O.J. II, Kirkman, K.L., and Peterson, R.S. (1981), "Sailing Yacht Capsizing," Proceedings of the Chesapeake Sailing Yacht Symposium, Annapolis, Maryland.

Tanaka, N. (1957-1961), "A Study on the Bilge Keel," (Parts 1-4), Journal of the Society of Naval Architects and Marine Engineers of Japan, Vol. 101, 103, 105, and 109.

Todd, F.N. (1963), "Series 60 Methodical Experiments With Models of Single-Screw Merchant Ships," DTMB Report 1712.

Tulin, M., and Mauro (1992), "Nonlinear Deck Wetness," presentation at Office of Naval Research Program Review Meeting, M.I.T., Cambridge, Massachusetts, (unpublished).

U.S. Coast Guard (1994), "*Italian Gold* Stability Analysis," Report 16710/P001353, November 1994.

Yue, D.K.P. (1994), "Program for Fully-Nonlinear Wave-Body Interactions," presented at ONR Workshop on the Nonlinear Ship Motions at DTRC.